

**CIRCUIT THEORETICAL METHODS FOR EFFICIENT  
SOLUTION OF FINITE ELEMENT STRUCTURAL  
MECHANICS PROBLEMS**

**A DISSERTATION  
SUBMITTED TO THE DEPARTMENT OF ELECTRICAL AND ELECTRONICS  
ENGINEERING  
AND THE INSTITUTE OF ENGINEERING AND SCIENCES  
OF BILKENT UNIVERSITY  
IN PARTIAL FULFILLMENT OF THE REQUIREMENTS  
FOR THE DEGREE OF  
DOCTOR OF PHILOSOPHY**

**By  
Ahmet Suet EKINCI**

**July 1999**

**TK  
454  
E35  
1999**

CIRCUIT THEORETICAL METHODS FOR EFFICIENT  
SOLUTION OF FINITE ELEMENT STRUCTURAL  
MECHANICS PROBLEMS

A DISSERTATION

SUBMITTED TO THE DEPARTMENT OF ELECTRICAL AND ELECTRONICS

ENGINEERING

AND THE INSTITUTE OF ENGINEERING AND SCIENCES

OF BILKENT UNIVERSITY

IN PARTIAL FULFILLMENT OF THE REQUIREMENTS

FOR THE DEGREE OF

DOCTOR OF PHILOSOPHY

By

Ahmet Suat Ekinci

July 6, 1999

TK  
454  
· E35  
1999

2049047

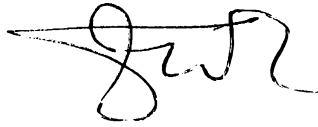
I certify that I have read this thesis and that in my opinion it is fully adequate, in scope and in quality, as a thesis for the degree of Doctor of Philosophy.



---

Abdullah Atalar, Ph. D. (Supervisor)

I certify that I have read this thesis and that in my opinion it is fully adequate, in scope and in quality, as a thesis for the degree of Doctor of Philosophy.



---

M. Erol Sezer, Ph. D.

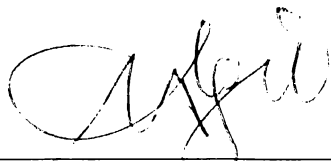
I certify that I have read this thesis and that in my opinion it is fully adequate, in scope and in quality, as a thesis for the degree of Doctor of Philosophy.



---

M. İrşadi Aksun, Ph. D.

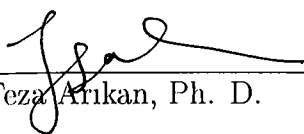
I certify that I have read this thesis and that in my opinion it is fully adequate, in scope and in quality, as a thesis for the degree of Doctor of Philosophy.



---

Mustafa Akgül, Ph. D.

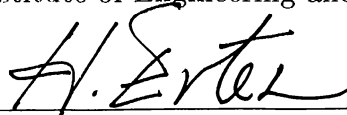
I certify that I have read this thesis and that in my opinion it is fully adequate, in scope and in quality, as a thesis for the degree of Doctor of Philosophy.



---

Feza Arıkan, Ph. D.

Approved for the Institute of Engineering and Sciences:



---

Prof. Dr. Mehmet Baray  
Director of Institute of Engineering and Sciences

## ABSTRACT

# CIRCUIT THEORETICAL METHODS FOR EFFICIENT SOLUTION OF FINITE ELEMENT STRUCTURAL MECHANICS PROBLEMS

Ahmet Suat Ekinçi

Ph. D. in Department of Electrical and Electronics Engineering

Supervisor: Prof. Dr. Abdullah Atalar

July 6, 1999

Shrinking device dimensions in integrated circuit technology made integrated circuits with millions of components a reality. As a result of this advance, electrical circuit simulators that can handle very large number of components have emerged. These programs use new circuit simulation techniques which approximate the system with reduced order models, and can find solutions accurately and quickly. This study proposes formulating the structural mechanics problems using FEM, and then employing the recent speedup techniques used in circuit simulation. This is obtained by generating an equivalent resistor-inductor-capacitor circuit containing controlled sources. We analyze the circuits with general-purpose circuit simulation programs, HSPICE, and an in-house developed circuit simulation program, MAWE, which makes use of generalized asymptotic waveform evaluation (AWE) technique. AWE is a moment matching technique that has been successfully used in circuit simulation for solutions of large sets of equations. Several examples on the analysis of the displacement distributions in rigid bodies have shown that using circuit simulators instead of conventional FEM solution methods improves simulation speed without a significant loss of accuracy. Pole analysis via congruence transformations (PACT) technique is a recent algorithm used for obtaining lower order models for large circuits. For a further reduction in time, we employed a similar algorithm in structural mechanics problems before obtaining the equivalent circuit. The results are very promising.

*Keywords:* Circuit Simulation, Asymptotic Waveform Evaluation (AWE), Pole Analysis via Congruence Transformations (PACT), Electrical Modeling.

## ÖZET

### YAPISAL MEKANİKTE SONLU ELEMAN PROBLEMLERİNİN HIZLI ÇÖZÜMÜ İÇİN DEVRE TEORİSİ YÖNTEMLERİ

Ahmet Suat Ekinci  
Elektrik ve Elektronik Mühendisliği Doktora  
Tez Yöneticisi: Prof. Dr. Abdullah Atalar  
6 Temmuz 1999

Tümleşik devre teknolojisinde küçülen eleman boyutları milyonlarca parçadan oluşan tümleşik devrelerin gerçekleştirilmesini sağladı. Bu gelişmenin sonucu olarak, çok yüksek sayıda parçayı ele alabilecek elektriksel devre benzetim yazılımları ortaya çıktı. Bu yazılımlar, sistemleri düşük dereceli modellerle yaklaştıran yeni benzetim yöntemlerini kullanmakta ve çözümleri doğru ve hızlı bir biçimde bulabilmektedir. Bu çalışma, yapısal mekanik problemlerinin sonlu eleman yöntemiyle formülize edilmesini ve sonra da devre benzetimlerinde kullanılan yeni hızlandırma yöntemlerinin uygulanmasını önermektedir. Bu, kontrollü kaynaklar da içeren eşdeğer direnç-irgiteç-sığaç devreleri oluşturularak sağlanmaktadır. Biz bu devreleri genel amaçlı devre benzeticileriyle; HSPICE ve geliştirilmiş asimptotsal eğri bulma (AEB) yöntemini kullanan, üniversitemizde geliştirilmiş MAWE yazılım programı ile, çözümledik. AEB devre benzetiminde büyük eşitlik kümelerinin çözümlerini bulmakta kullanılan bir moment eşleme tekniğidir. Yapılan çeşitli sert kitlelerdeki yerdeğiştirme dağılımı çözümleri, geleneksel sonlu eleman yöntemi çözümlerinin yerine devre benzeticilerinin kullanılmasının doğruluktan kaybetmeden benzetim hızında ilerleme sağlandığını göstermiştir. Eşleşik dönüşümlerle kutup analizi, devreler için düşük dereceli modeller bulunmasında kullanılan yeni bir yöntemdir. Zamanda daha fazla bir kısalma sağlamak için, yapısal mekanik problemlerinde eşdeğer devre bulmadan önce bu yöntemle benzer bir algoritma kullandık. Sonuçlar gelecek için çok iyi şeyler vaadediyor.

*Anahtar Kelimeler:* Devre Benzetimi, Asimptotsal Eğri Bulma Yöntemi, Eşleşik Dönüşümlerle Kutup Analizi, Elektriksel Modelleme.

## ACKNOWLEDGMENTS

I would like to express my deep gratitude to my supervisor Dr. Abdullah Atalar for his guidance, suggestions and encouragement in all steps of the development of this work.

I would like to thank Dr. Erol Sezer, Dr. İřadi Aksun, Dr. Mustafa Akgül and Dr. Feza Arıkan for their motivating and directive comments on my research. Also special thanks to Dr. Mustafa Karaman and Dr. Cevdet Aykanat for commenting on the previous manuscripts.

It is a pleasure for me to express my thanks to Mustafa Yazgan for his valuable discussions.

Special thanks to my friends Sanli Ergun, Ayhan Bozkurt, Ömer Gerek, Alper Kutay, Tolga Yalçın, Dicle Öziř and Mithat Ünsal for their moral support and friendship.

Finally, I would like to thank my father, mother and sister for their continuous support throughout my graduate study.



# Contents

<b>1</b>	<b>Introduction</b>	<b>1</b>
<b>2</b>	<b>Finite Element Formulation</b>	<b>6</b>
2.1	Finite Element Method . . . . .	7
<b>3</b>	<b>Electrical Circuit Simulation</b>	<b>11</b>
3.1	Overview of Moment-matching Techniques . . . . .	12
3.1.1	Generation of the Moments	13
3.1.2	Asymptotic Waveform Evaluation (AWE), Complex Frequency Hop- ping (CFH) and MAWE . . . . .	13
<b>4</b>	<b>Equivalent circuit extraction</b>	<b>16</b>
4.1	Method I . . . . .	19
4.2	Method II . . . . .	19
4.3	Example . . . . .	20
<b>5</b>	<b>PACT algorithm for mechanical problems</b>	<b>22</b>

<b>6</b>	<b>Examples</b>	<b>30</b>
6.1	Example I . . . . .	30
6.2	Example II	33
6.3	Example III . . . . .	35
6.4	Example IV	37
6.5	Example V	41
6.6	Example VI	45
<b>7</b>	<b>Conclusions</b>	<b>50</b>
<b>A</b>	<b>Lagrange's Equations</b>	<b>53</b>
A.1	Generalized Coordinates . . . . .	53
A.2	Constraints	54
A.3	Virtual Work	54
A.4	Constraint Forces . . . . .	55
A.5	The Principle of Virtual Work . . . . .	55
A.6	D'Alembert's Principle . . . . .	56
A.7	Generalized Forces	56
A.8	Lagrange's Equations . . . . .	57
<b>B</b>	<b>Modal Superposition</b>	<b>60</b>
<b>C</b>	<b>Modified Node Analysis Formulation</b>	<b>62</b>

<b>D Matlab Codes for PACT</b>	<b>64</b>
D.1 PACT	64
D.2 $LDL^T$	70
D.3 Lanczos Process . . . . .	73
D.4 Solution . . . . .	75
D.5 Sample Run . . . . .	76
D.5.1 Structural Analysis . . . . .	76
D.5.2 Circuit Simulation	77
<b>Vita</b>	<b>85</b>

# List of Figures

4.1	Two-mass-spring system . . . . .	20
4.2	Equivalent circuit for the two-spring-mass system . . . . .	21
6.1	Four spring-mass system. (Example I)	31
6.2	Equivalent electrical circuit for a single damped spring-mass system.	32
6.3	Transient analysis results for Example I.	32
6.4	Bar supported at the two sides (Example II).	33
6.5	Harmonic analysis results for Example II.	34
6.6	Transient analysis results of the three methods for Example III.	36
6.7	Simply supported thin annular plate (Example IV). . . . .	37
6.8	Harmonic analysis results around the missing pole in Example IV.	38
6.9	Harmonic analysis results around the missing pole in Example IV.	38
6.10	Harmonic analysis results of the three methods for Example IV.	40
6.11	Solid square plate supported at one edge (Example V). . . . .	41
6.12	Harmonic analysis results of the three methods for Example V.	43

6.13 More accurate harmonic analysis results for Example V. The pole at 132.88 Hz can only be found by MAWE.	43
6.14 Harmonic analysis result using PACT.	44
6.15 The sketch of the problem in Example VI.	45
6.16 The displacement and velocity propagation in the long bar of Example VI.	47
6.17 Comparison of the results obtained using the three simulators (0.24 sec).	48
6.18 Comparison of the results obtained using the three simulators (1 sec).	49
C.1 Symbols for the electrical circuit elements	63

# List of Tables

2.1	Equations in structural problems	7
6.1	Circuit summary for Example II.	33
6.2	Timing results for Example II (entries are in seconds).	35
6.3	Timing results of the transient analysis in Example III (in seconds).	36
6.4	Timing results for Example IV. (Seconds)	39
6.5	Evaluation point-number of moments pairs (Example V).	42
6.6	Evaluation point-number of moments pairs for reduced circuit.	44
6.7	Timing results for Example V (times are in seconds). . . . .	45
C.1	Branch equations for the circuit elements	63

# Chapter 1

## Introduction

Finite element method, which is used for finding an approximate solution for problems, has found extensive applicability in the field of structural mechanics. This method has now become a predominant analysis and design tool.

Finite element formulations result in large sets of equations. Space/frequency formulations involve the solution of the large system at many frequency points or require the computationally expensive process of determining eigenvalues and corresponding eigenvectors of large matrices.

In both structural mechanics problems and electrical circuit simulation problems we meet similar types of analyses; namely steady state (or time independent) analysis, eigenvalue analysis, and propagation (or transient) analysis.

The electrical circuit simulation programs employ different methods to find the circuit behaviour. Spice-like programs [1-3] are used for intensive verification of large circuits and find high accuracy solutions. In these programs the inverse of the matrix is calculated at a large number of points in both frequency and time domains. However, most of the new simulators involve smaller number of matrix solutions.

Asymptotic waveform evaluation [4] (AWE) technique is widely used in the simulation of very large circuits. In this method, the system behaviour is approximated with a lower order model. The method is based on the Taylor series expansion of the circuit response around  $s = 0$ , and it is very efficient to extract the low frequency behaviour of the circuit.

To find the behaviour in a frequency range of interest, which does not contain only the low frequency region, complex frequency hopping (CFH) technique is introduced [5]; and recently a multi-point Padé-approximation technique is developed [6, 7]. In these studies, the expansions for different frequency points are found. The multi-point moment matching method may also be extended to use the information of expansions at infinity [8]. This information is basically needed to approximate the transient behaviour.

Several studies have been done to use the simplicity of the circuit solution techniques in the field analysis problems. G. Kron suggested equivalent circuits of the elastic fields [9], and G. K. Carter dealt with the solution techniques of these circuits [10]. In those circuits, the stresses are represented by currents and the strains by voltages. Electrical equivalents of the equations are obtained and satisfied by the equivalent networks.

In the recent years, electrical thermal network analogy is widely used to study thermal behaviour of electronic components, and the analogy leads to large resistor-capacitor (RC) networks which are analyzed by using circuit simulation techniques. In the work of Hsu et. al., elemental thermal circuit networks, which correspond to elements in 1-D, 2-D and 3-D cases are developed [11]. These networks are connected to the electrical networks to provide complete electro-thermal models that can be used in any circuit simulation packages. Same authors also studied model order reduction techniques for large problems [12] in electro-thermal analysis.

There are studies on coupling the external circuit equations with finite element models. These studies can be classified into two different approaches: the equations of the



finite element model and circuit model may be handled as a single system of equations [13–17], or finite element part may be handled as a separate system which communicates with the circuit model [18–21]. The first approach is called direct coupling and the second is called indirect coupling. Direct coupling is popular, because quite effective and reliably convergent computation is possible by applying Newton-Raphson iteration on the combined problem. Usually the number of nodes in finite element mesh is so large that sparse matrix methods have to be used, but the combination of the models change the sparsity and symmetry of the finite element matrices. In indirect coupling, the finite element model is handled separately [19–21]. In the works of Väänänen [19] and McDermott et. al. [21] the parts modeled by the finite element method are considered as a multiport element in the circuit. Both of these works require the solution of the finite element model first.

Transmission line modeling [22] is also used in stress-strain analysis problems, but it is difficult to handle the analysis of transmission lines. Another disadvantage of such modeling is the introduction of voltage source inductor loops which have to be solved using special techniques. AWE technique in circuits containing transmission lines is not as efficient as in the RLC circuits because of the extra multiplications in moment updating procedure.

Recently, techniques mainly developed for circuit simulation are used in the solution of electromagnetic analysis problems. AWE is proposed in the study by Gong [23], where the reduction of the order of the parameters, such as input impedance, S parameters, and far field pattern using a new moment update procedure is discussed. In the work of Kolbehdari, CFH technique is studied [24]. In CFH technique frequency range is divided into regions and the response is approximated by different transfer functions at each frequency region. Both studies show that usage of circuit simulation techniques is promising.

Most of the new techniques for Pade based model order reduction employ Krylov

subspace methods. The Lanczos algorithm and the Arnoldi process have long been recognized as powerful tools for large scale matrix computations. Krylov subspace methods [25] involve the matrix only in the form of matrix-vector products with matrix or its transpose, and have become standard tools for iterative solutions of large systems of linear equations and for large scale eigenvalue computations [26]. Krylov subspace methods are also adapted to solve the problems for structural systems [27–31].

There is a recent increase of interest in Krylov-subspace methods for reduced order modeling because of the need of such simulation techniques in the simulation of integrated electronic circuits. Feldmann and Freund used the Lanczos connection of Padé approximation to obtain high order Padé approximations in circuit simulation [32]. The numerical problems of AWE can be remedied by using Lanczos process. This approach is called PVL. For single-input single-output RLC circuits, the symmetry of the transfer functions can be exploited by employing a symmetric version of Lanczos algorithm. The SyPVL is introduced in [33].

The PVL approach is generalized to multi-input multi-output case by the same authors [34] where the method is developed in [35]. The symmetric version of the algorithm (SyMPVL), for the computation of multiport transfer functions of RLC circuits is described in manuscripts [36] and [37].

It is desirable that reduced order models inherit the essential properties of the original linear dynamical systems. These properties are stability and passivity. SyMPVL does not guarantee passivity, but it can be changed to give passive reduced order models which match half as many moments as the Padé approximation of the same order. Recently, Odabasioglu [38] developed an Arnoldi based reduced order modeling technique which preserves passivity.

For RC circuits, a different Padé-based reduced order modeling technique, the PACT algorithm, was proposed [39]. Here one block of circuit variables is eliminated in the transfer function. The result has a smaller state-space dimension. The algorithm gives a

passive reduced order model and is efficient when the number of network ports is large. An extension of the method, for RLC circuits, based on split-congruence transformation is studied by the same authors [40].

In [41], R.W. Freund reviews main ideas of reduced order modeling techniques based on Krylov subspaces and their usage in circuit modeling.

The model order reduction methods for structural mechanics employ Modal Superposition(MS) and Component Mode Synthesis(CMS) methods [12]. In MS, the eigenvalues and eigenvectors of the system are obtained. Using the information from the dominant ones the equations are made uncoupled, and the problem is solved easily. The idea of CMS method is to find reduced models for various structures independently, and to use compatibility conditions to connect these reduced substructure models.

In this thesis, we studied electrical circuit simulation methods in the solutions of structural mechanics problems modeled using finite element method. We introduced a technique to obtain an equivalent electrical circuit for a structure. Solving the circuit using general purpose circuit simulators, HSPICE [3] and MAWE [7], we obtained a great speedup. For a further increase in simulation efficiency we developed a model order reduction algorithm based on both PACT algorithm and Krylov subspace methods. Using this technique we first find a reduced order model, then we obtain the equivalent circuit.

# Chapter 2

## Finite Element Formulation

In a typical structural analysis, we try to find the stress and displacement distribution in a rigid body under a set of loading and boundary conditions. The following equations have to be solved to find an analytical solution of the problem.

$$\tilde{\nabla}_s \cdot \mathbf{T} = \rho \frac{\partial \mathbf{v}}{\partial t} - \mathbf{F} \quad (2.1)$$

$$\mathbf{T} = \mathbf{c} : \mathbf{S} \quad (2.2)$$

$$\mathbf{S} = \nabla_s \mathbf{u} \quad (2.3)$$

In these equations the following notation is used:

$\mathbf{u}$  : Displacement vector  $(u_x, u_y, u_z)$ ,

$\mathbf{v}$  : velocity vector  $(v_x, v_y, v_z)$ ,

$\mathbf{S}$  : Strain tensor  $(S_1 = S_{xx}, S_2 = S_{yy}, S_3 = S_{zz}, S_4 = S_{yz}, S_5 = S_{xz}, S_6 = S_{xy})$ ,

$\mathbf{T}$  : Stress tensor  $(T_1 = T_{xx}, T_2 = T_{yy}, T_3 = T_{zz}, T_4 = T_{yz}, T_5 = T_{xz}, T_6 = T_{xy})$ ,

$\mathbf{c}$  : elastic stiffness matrix

$\rho$  : mass density

Table 2.1: Equations (1),(2),(3) and unknowns in structural problems.

type of equations	number of equations	unknowns	number of unknowns
Translational eqn. of motion	3	Displacement	3
Stress-strain relation	6	Stress	6
Strain-displacement relations	6	Strain	6
Total	15	Total	15

In the equations “ $\nabla_s$ ” corresponds to an operator represented by the following matrix:

$$\nabla_s \rightarrow \begin{bmatrix} \partial/\partial x & 0 & 0 \\ 0 & \partial/\partial y & 0 \\ 0 & 0 & \partial/\partial z \\ 0 & \partial/\partial z & \partial/\partial y \\ \partial/\partial z & 0 & \partial/\partial x \\ \partial/\partial y & \partial/\partial x & 0 \end{bmatrix}$$

and “ $\tilde{\nabla}_s$ ” corresponds to the operator represented by the transpose of the same matrix. Velocity, the time derivative of displacement; i.e.,  $v = \frac{\partial u}{\partial t}$ , is also used. Table 2.1 shows the equations and unknowns.

In practice, equations known as compatibility equations (continuity of strains and displacements), and boundary conditions (conditions on displacements, forces at the boundary) also have to be satisfied.

## 2.1 Finite Element Method

Finite Element method is used to find an approximate solution of the problem. In the literature, displacement method or the minimum potential approach have been extensively used. In this method, all the equations are written in terms of the displacement

components and solved for unknown displacements. We will give a brief flow of algorithm [42–44] for the dynamical systems in order to make the analogy between the structural problems and the electrical circuit problems clear.

Let the body be meshed into  $E$  elements. The displacement model of the  $e^{\text{th}}$  element is denoted as :

$$\vec{u}^{(e)}(x, y, z, t) = \begin{Bmatrix} u_x^{(e)}(x, y, z, t) \\ u_y^{(e)}(x, y, z, t) \\ u_z^{(e)}(x, y, z, t) \end{Bmatrix} = \mathbf{N}(x, y, z) \vec{Q}^{(e)}(t) \quad (2.4)$$

Where  $\vec{u}^{(e)}$  is the vector of displacement,  $\mathbf{N}$  is the matrix of shape functions,  $\vec{Q}^{(e)}$  is the vector of degrees of freedom and is assumed to be a function of time  $t$ .

Using (2.3) with  $\mathbf{B} = \nabla_s \mathbf{N}$ , the strains can be approximated as

$$\mathbf{S}^{(e)} = \mathbf{B} \vec{Q}^{(e)} \quad (2.5)$$

and stresses as

$$\mathbf{T}^{(e)} = \mathbf{c} : \mathbf{S}^{(e)} = \mathbf{cB} \vec{Q}^{(e)} \quad (2.6)$$

The kinetic energy  $\pi_k$  and the potential energy  $\pi_p$  can be expressed as:

$$\pi_k = \sum_{e=1}^E \pi_k^{(e)} = \frac{1}{2} \dot{\vec{\mathbf{Q}}}^T \left[ \sum_{e=1}^E \int \int \int_{V^{(e)}} \rho \mathbf{N}^T \mathbf{N} \, dV \right] \dot{\vec{\mathbf{Q}}} \quad (2.7)$$

where  $[\cdot]^T$  denotes the transpose of the matrices and the vectors, and  $\dot{\vec{\mathbf{Q}}}$  denotes the time derivative.

$$\pi_p = \sum_{e=1}^E \pi_p^{(e)} = \frac{1}{2} \vec{\mathbf{Q}}^T \left[ \sum_{e=1}^E \int \int \int_{V^{(e)}} \mathbf{B}^T \mathbf{c} \mathbf{B} \, dV \right] \vec{\mathbf{Q}} - \vec{\mathbf{Q}}^T \vec{\mathbf{P}}(t) \quad (2.8)$$

where  $\vec{\mathbf{P}}(t)$  is the total load vector

Matrices  $\mathbf{M}$ , master mass matrix of the structure; and  $\mathbf{K}$ , master stiffness matrix of the

structure, are defined as:

$$\begin{aligned}\mathbf{M} &= \sum_{e=1}^E \int \int \int_{V^{(e)}} \rho \mathbf{N}^T \mathbf{N} \, dV \\ \mathbf{K} &= \sum_{e=1}^E \int \int \int_{V^{(e)}} \mathbf{B}^T \mathbf{c} \mathbf{B} \, dV\end{aligned}\quad (2.9)$$

Using a modified form of Lagrange's equations [45],

$$\frac{d}{dt} \left\{ \frac{\partial L}{\partial \dot{Q}_i} \right\} - \frac{\partial L}{\partial Q_i} + \frac{\partial R}{\partial \dot{Q}_i} = 0 \quad i = 1, 2, \dots, n \quad (2.10)$$

where  $L = \pi_k - \pi_p$  is the Lagrangian,  $n$  is the number of unknowns and  $R$  stands for the dissipation. we obtain the desired dynamic equations of motion of the structure.

$$\mathbf{M}\ddot{\vec{Q}}(t) + \mathbf{C}\dot{\vec{Q}}(t) + \mathbf{K}\vec{Q}(t) = \vec{P}(t) \quad (2.11)$$

$\mathbf{C}$  is the master damping matrix of the structure, and it is usually defined as

$$\mathbf{C} = \alpha\mathbf{M} + \beta\mathbf{K} + \mathbf{C}_\xi \quad (2.12)$$

where  $\alpha$  and  $\beta$  are constants, and  $\mathbf{C}_\xi$  is the frequency dependent damping matrix. If damping is neglected, we have the lossless case:

$$\mathbf{M}\ddot{\vec{Q}}(t) + \mathbf{K}\vec{Q}(t) = \vec{P}(t) \quad (2.13)$$

Equations (2.11) and (2.13) can be solved using different mathematical techniques, once the vector  $\vec{Q}(t)$  is known, the variations of the displacements, stresses and strains in the elements can be found.

Various kinds of analysis of dynamical systems can be done using the equation of motion.

If the aim of the stress analysis or solid mechanics problems is to find the distribution of displacements and stresses under the stated loading and boundary conditions, there will be no time dependency, so the equation becomes:

$$\mathbf{K}\vec{Q} = \vec{P}$$

In transient analysis all the unknowns are time-dependent, and the equation of motion has to be solved. Generally, the finite difference method or Newmark's method is used to find the solution.

The frequency behaviour of the structure can be found using harmonic analysis. The displacements are assumed to be harmonic as

$$\vec{\mathbf{Q}}(t) = \vec{\mathbf{Q}}e^{j\omega t}$$

where  $j = \sqrt{-1}$  and the equation becomes

$$\left[-\omega^2\mathbf{M} + j\omega\mathbf{C} + \mathbf{K}\right] \vec{\mathbf{Q}} = \vec{\mathbf{P}} \quad (2.14)$$

The oscillatory motion occurs at certain frequencies known as natural frequencies or characteristic values, and follows well defined deformation patterns known as mode shapes or characteristic modes. The natural frequencies and mode shapes can be found using eigenvalue analysis techniques. The modes are the eigenvalues of the system defined by the equation (2.14).



## Chapter 3

# Electrical Circuit Simulation

Today's integrated circuits are extremely complex, with up to millions of devices, this makes computational methods to simulate and analyze the behaviour of the circuit at the design stage very important. The first crucial issue in circuit simulation is the modeling of the circuit. Most of the recent electrical circuit simulators use Modified Node Analysis (MNA) formulation to build the circuit matrices, as it introduces less redundancy than other methods.

For linear electrical circuits MNA formulation gives the following equation system [46]:

$$\mathbf{C} \dot{x} = -\mathbf{G} x + \mathbf{b}u(t) \quad (3.1)$$

where  $\mathbf{C}$  is the matrix of capacitances and inductors,  $\mathbf{G}$  is the admittance matrix,  $u(t)$  is the voltage or current excitation at the nodes defined by vector  $\mathbf{b}$ , and the unknown state vector  $x$  contains nodal voltages, inductor currents and voltage supply currents. The set of the equations come from the modified node analysis. In Appendix C, modified node analysis formulation is described, and the current voltage relations of the electrical circuit components which we use in this study are shown.

In transient analysis, time variations of the state variables, the entries of the vector

$x$ , are found. In AC analysis the frequency response of the system is investigated. i.e., the equation

$$(\mathbf{G} + s\mathbf{C}) X(s) = \mathbf{b}U(s) \quad (3.2)$$

is solved. Frequency response is obtained at  $s = j\omega$  ( $j = \sqrt{-1}$ ).

In pole-zero analysis, the eigenvalues of the system defined by the equation (3.2) are found.

The dynamic equation of motion (2.11) which is a second order differential equation can be converted into an equation of order one [43], so that it will be the same as the circuit equation (3.1) and it can be solved using circuit simulation techniques.

The shrinking of the circuit sizes makes it possible to build larger circuits which results in large systems of equations. Since the direct solutions of such systems will take a lot of time, the circuit simulation techniques are improved in order to handle the analysis. New methods for faster analysis are developed without losing the accuracy.

### 3.1 Overview of Moment-matching Techniques

The moment-matching techniques are widely used in circuit simulation in order to reduce the execution time [4-7,47-51]. In these techniques by approximating the dominant poles of the circuit with a lower order model, the behaviour of the circuit is obtained.

Moment-matching uses the coefficients (moments) of the expansion of the system transfer function,  $H(s)$ , around a point in the complex  $s$ -plane. The Taylor series expansion of  $H(s)$  around  $s_0$  is given as:

$$H(s) = m_0 + (s - s_0)m_1 + (s - s_0)^2m_2 + \dots \quad (3.3)$$

After the moments are generated, they are matched to a ratio of two polynomials [4, 6, 7] or to a low-order set of poles and residues [5] by using Padé approximation.

### 3.1.1 Generation of the Moments

The transfer function for a circuit which consists of lumped elements is (using Equation 3.2)

$$H(s) = (\mathbf{G} + s\mathbf{C})^{-1}\mathbf{b} \quad (3.4)$$

or with a change of variable  $s = s_0 + \sigma$

$$H(s_0 + \sigma) = (\mathbf{I} + \sigma(\mathbf{G} + s_0\mathbf{C})^{-1}\mathbf{C})^{-1}(\mathbf{G} + s_0\mathbf{C})^{-1}\mathbf{b} \quad (3.5)$$

The transfer function is approximated (for small  $\sigma$ ) as

$$\hat{H}(\sigma) = (\mathbf{I} + \sigma\mathbf{A} + \sigma^2\mathbf{A}^2 + \cdots + \sigma^n\mathbf{A}^n)\mathbf{r}$$

where

$$\begin{aligned} s &= s_0 + \sigma \\ \mathbf{A} &= -(\mathbf{G} + s_0\mathbf{C})^{-1}\mathbf{C} \\ \mathbf{r} &= (\mathbf{G} + s_0\mathbf{C})^{-1}\mathbf{b} \end{aligned}$$

As a result the moments are found using  $m_n = \mathbf{A}^n\mathbf{r}$ . During the generation of moments the LU decomposition of the circuit matrix is calculated once for the first moment. Other moments are obtained using forward and backward substitutions.

In transient analysis, Laurent series expansion ( $s = \infty$ ) may also be used [5,48-50,52]. These moments are called the derivative moments, because they are the derivatives of the time response [49,51].

### 3.1.2 Asymptotic Waveform Evaluation (AWE), Complex Frequency Hopping (CFH) and MAWE

In asymptotic waveform evaluation technique, to approximate the behaviour of the circuit, the Taylor expansion around  $s = 0$  is evaluated. Since the information carried

by the moments is accurate at low frequency region, the AWE technique is efficient in extracting the low frequency poles of the circuit. At relatively higher frequencies the AWE technique becomes inefficient and several methods are proposed to improve the accuracy of AWE.

After the moments are generated, the transfer function is approximated with a rational function.

$$\begin{aligned}\hat{H}(s) &= m_0 + m_1s + m_2s^2 + \dots + m_ns^n \\ &= \frac{B(s)}{A(s)} = \frac{\sum_{i=0}^p b_i s^i}{\sum_{j=0}^q a_j s^j}\end{aligned}\quad (3.6)$$

$$= \sum_{i=1}^q \frac{k_i}{s - p_i}\quad (3.7)$$

where  $p_i$ 's are the poles and  $k_i$ 's are the corresponding residues. The methods to calculate the coefficients are documented in literature [4, 47, 50]. First the coefficients  $a_i$  are found by setting up a moment matrix, then poles and finally residues are calculated.

When the moments at  $s = \infty$  are also included, a single moment matrix is set up again, and solved for the poles. Therefore the method is referred to as single-point Padé approximation.

Recently, multi-point Padé approximation techniques were proposed [5-7]. In the work by Chiprout et. al. [5] complex frequency hopping (CFH) technique is introduced. The transfer function  $H(s)$  is expanded around  $s = 0$  and  $s = j\omega_{max}$ , and a binary search algorithm is employed until two neighbour expansions have a pole in common. Using these common poles, a region of accuracy is assigned for each expansion point. The poles in the region of accuracy and their corresponding residues are marked as accurate. The final estimate of transfer function contains all the marked poles and residues.

In the works of Celik et. al. [6] and Sungur et. al. [7] moment matching is done by simultaneously solving all the moment matrices obtained at each expansion. MAWE circuit simulation tool uses this method.

In finding circuit transfer functions, we usually choose  $p = q - 1$  in equation (3.6). This rational approximation is referred to as Padé approximation of order  $q$ . The method that we use for finding the coefficients,  $a_i$  and  $b_i$ , is described in detail in the study by Sungur et. al. [7].

The multi-point Padé approximation works not only for low frequencies, but also in high frequency regions. Apart from the moments at  $s = 0$  (DC), the use of shifted moments provides the necessary information about the frequency range of interest. This approach requires the solution of the circuit matrix at several frequency points.

Padé approximation technique is very efficient in transient analysis. After obtaining the poles and residues of the system, the inverse transform; i.e., impulse response can be found easily.

When the number of poles in the problem is large, the approximation order should be large. This can be achieved by increasing the number of calculated moments, but this may give ill-conditioned moment-matrices. To have a stable solution, 8-16 moments have to be evaluated at each expansion point. Therefore, higher order approximations can be reached by increasing the expansion points which means increasing the number of LU decompositions.

# Chapter 4

## Equivalent circuit extraction

Equivalent circuit approach is used to simulate the behaviour of a system with a simpler model or to solve coupled field-circuit problems. There are recent studies on electro-thermal [11], electromechanical [21] and electromagnetic [19] problems which present procedures to build equivalent circuits.

In the work of McDermott et. al. [21] the behavioral model of the electromechanical devices is extracted from a set of parametric finite element solutions. A new circuit element (a piecewise linear dependent source) is introduced. This component uses a lookup table produced by the FEM solutions. For example, given position and current, it returns flux and force.

In the work of Väänänen [19] the finite element model is handled as a circuit theoretical multiport element. In the FE model, unknowns other than the coupled potentials and currents are eliminated and a matrix equation for these electrical unknowns is derived. The problem is discretized in time so that the solution of a time-dependent problem is converted into successive solutions of a DC problem. The final equations are treated as electrical circuit equations and the FE model is represented by a multiport element containing current controlled current sources (CCCS), voltage controlled current

sources (VCCS), voltage controlled voltage sources (VCVS) and current controlled voltage sources (CCVS). This method can handle nonlinearities by updating the multiport electrical circuit parameters at each iteration.

The methods mentioned in the two works require the solution of FE model which takes a lot of time. However, in this study we want to demonstrate that the efficiency of the electrical circuit simulation techniques can be applicable to FE models.

In the study performed by Hsu et. al. [11], thermal circuit networks, which are equivalent to discretization of the heat equation by FEM, are developed. Elemental thermal circuit networks are constructed for 1-D, 2-D and 3-D elements. The semi-discrete heat equation (continuous in time) derived from a Galerkin finite element projection [11] is:

$$\mathbf{M}\dot{\mathbf{d}} + \mathbf{K}\mathbf{d} = \mathbf{F} \quad (4.1)$$

It is easily seen that the mass matrix  $\mathbf{M}$  can be realized using capacitor elements, the stiffness matrix  $\mathbf{K}$  by resistor elements and the force vector  $\mathbf{F}$  by current sources. The procedure for deriving the equivalent circuits is given in the article. The simulations were performed using SABER [53] circuit simulator where the thermal networks are written as element templates. This method is useful for field-circuit coupled problems, e.g. simulation of self-heating effects in semiconductor devices.

The works summarized up to now are suggested to solve the coupled field-circuit problems. While the first two methods require the simulation of the FE model, throughout the procedure in the last method no matrix inversion, or decomposition is needed. However, this method may introduce negative values for capacitances and resistors, and this is not acceptable in a general circuit simulation tool. In this study, we propose a method which does not need any matrix inversion in the circuit construction procedure. The final circuit can be solved using a general circuit simulator, and fast methods developed for simulation of electrical circuits can be used.

The method suggested by Hsu et. al. [11] can be generalized for use with second

order equations. One can realize matrices  $\mathbf{M}$ ,  $\mathbf{C}$ ,  $\mathbf{K}$  in equation (2.11) by capacitances, resistances and inductances respectively, and the force vector  $\vec{\mathbf{P}}$  by current sources. Here the problem of negative valued elements also arise, but there are more serious problems. For lossless case, inductor loops may occur and such circuits have to be solved using special techniques. For each nondiagonal entry in the stiffness matrix an inductor is placed into circuit which introduces an other unknown (inductor current) in the MNA formulation. If the total number of entries in the stiffness matrix  $\mathbf{K}$  is  $n \times n$  the circuit matrices in MNA formulation may go up to  $(\frac{\alpha}{2}n^2) \times (\frac{\alpha}{2}n^2)$ , where  $\alpha$  is the density of sparse stiffness matrix.

In our study the first step is to change the second order differential equation (2.11) into a first order differential equation.

$$\left[ \begin{array}{c|c} \mathbf{I} & \mathbf{0} \\ \hline \mathbf{0} & \mathbf{M} \end{array} \right] \cdot \dot{\mathbf{y}} = - \left[ \begin{array}{c|c} \mathbf{0} & -\mathbf{I} \\ \hline \mathbf{K} & \mathbf{C} \end{array} \right] \cdot \mathbf{y} + \left[ \begin{array}{c} \mathbf{0} \\ \mathbf{P} \end{array} \right] \quad (4.2)$$

where  $\mathbf{I}$  is the identity matrix, and

$$\mathbf{y} = \left[ \begin{array}{c} \vec{\mathbf{Q}}(t) \\ \dot{\vec{\mathbf{Q}}}(t) \end{array} \right]$$

Equation(4.2) is similar to the circuit equations (3.1); but the circuit matrices are positive on the diagonal.

To construct the equivalent circuit we developed two similar methods for the lossless case. These methods are of order  $N^2$ , and the conversion time is very small compared to the simulation time.

The difference of the methods is the choice of the unknowns which corresponds to  $\vec{\mathbf{Q}}(t)$ . The extracted circuits have MNA matrices larger than the original FEM problem.



## 4.1 Method I

In the first method, the displacements are chosen as node voltages. Such a choice leads us to choose the velocities as currents through capacitors. This means that there will be one capacitor for each unknown displacement. The other entries are realized using *voltage controlled voltage sources* and inductors. These are the effects of the displacements in the neighbour elements. The force effects are handled using voltage supplies. For the damped case we also need *current controlled voltage sources* to simulate the entries of damping matrix.

In this method every coupling introduces a series branch, which means an addition of two rows to the circuit matrix; one for the additional node voltage and one for the branch current, so the matrix may become very large.

## 4.2 Method II

Another choice, where the velocities correspond to the node voltages, gives the currents through the inductors as displacements. There is also a capacitor in parallel for each unknown displacement. The other entries are simulated using *current controlled current sources (CCCS)*. For the damped case we introduce *voltage controlled current sources*.

All the circuit elements come in parallel so that no additional equations are needed, but to couple the currents one needs to add zero-volt voltage supplies. The loads at the finite element nodes are realized using current sources.

For each displacement-velocity pair, there are 6 rows in the circuit matrix. Although the size of the matrix defining the linear system is 6 times the original matrix size, the number of entries does not grow much. The number of entries becomes  $2\alpha n^2 + 12n$  where  $\alpha$  is the density of the sparse,  $n \times n$ , stiffness and mass matrices. So the density of the

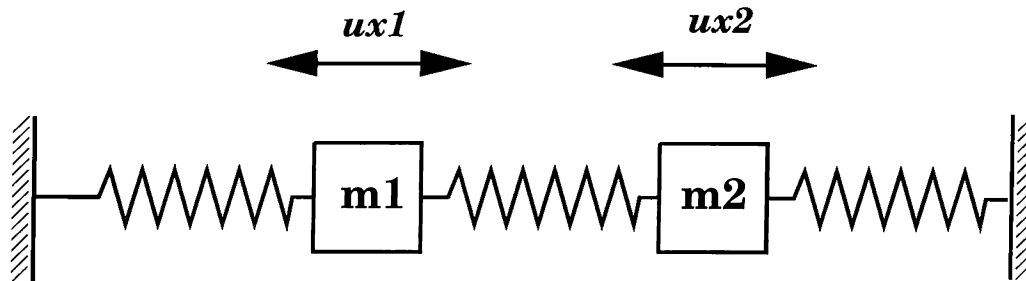


Figure 4.1: Two-mass-spring system

circuit matrix will be about  $2n^2\alpha/(6n)^2 = \frac{1}{18}\alpha$ .

### 4.3 Example

In this example we consider the analysis of a very simple two-mass-spring system shown in Fig. 4.1.

The analysis is done to find the modes of the system. There are only two unknowns  $ux1$  and  $ux2$ . In finite element formulation **M** and **K** matrices are  $2 \times 2$ .

The equivalent electrical circuits are shown in Fig. 4.2. The upper circuit is obtained using Method I, and the lower circuit is extracted using Method II. In the first circuit the voltages,  $v_{C1}$  and  $v_{C2}$  across the capacitors **C1** and **C2** correspond to the unknown displacements  $ux1$  and  $ux2$  respectively. The circuit has 6 node equations and 6 branch current equations, so the equivalent circuit matrix is  $12 \times 12$ . In the second circuit the currents,  $i_{L1}$  and  $i_{L2}$ , through the inductors **L1** and **L2** correspond to the unknown displacements. This circuit has also 6 equations for the node voltages and 6 equations for the branch currents, and the matrix of the equivalent circuit is again  $12 \times 12$ .

In finite element analysis the natural frequencies are found to be 2.5814 Hz and 8.3263 Hz. The equivalent circuits have poles at exactly the same frequencies. For this very simple example, the analysis times for the finite element solver and the circuit simulator

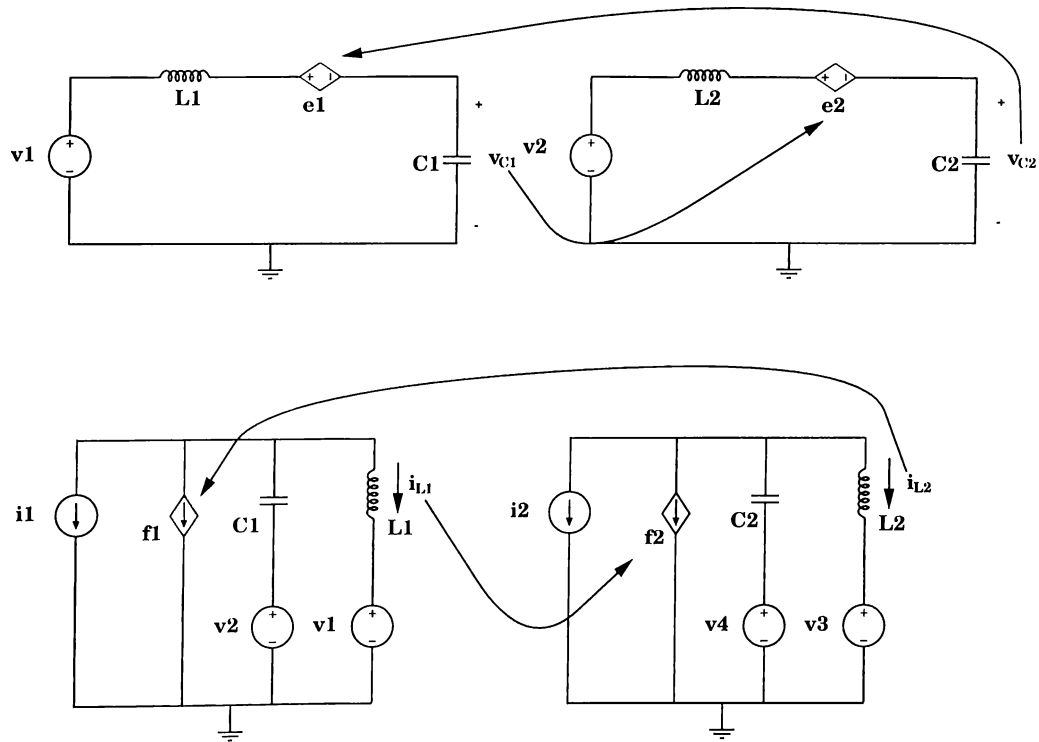


Figure 4.2: Equivalent circuit for the two-spring-mass system

MAWE are comparable (0.25 and 0.13 seconds). Only one expansion point is enough as it is a small circuit.

# Chapter 5

## PACT algorithm for mechanical problems

Practical problems usually lead to very large systems of equations. To increase the efficiency of electrical circuit techniques, model order reduction techniques may be used. In this study, we use Padé approximation to obtain reduced order models of the circuit.

For structural mechanics problems, two model order reduction techniques had been developed : Modal Superposition(MS) and Component Mode Synthesis(CMS). In MS the dominant modes of the system are obtained, and all the behaviors of the system are modeled as a combination of these modes. In CMS, reduced models of various substructures are obtained and connected using compatibility relations. MS method is described in Appendix B.

Pole analysis via congruence transformations(PACT) is a recent technique developed for efficient solution of RC circuits [39]. The idea is similar to CMS method, the circuit nodes are separated as port nodes and internal nodes. The internal nodes are eliminated and are replaced with a reduced order model. We generalized PACT algorithm to structural mechanics problems. As the second step of algorithm, to obtain a reduced order

model we employed Lanczos process instead of pole analysis.

In this chapter we give the flow of generalized PACT algorithm.

The equation of motion is

$$s^2\mathbf{M}x + s\mathbf{C}x + \mathbf{K}x = \mathbf{F} \quad (5.1)$$

where  $\mathbf{C} = \alpha\mathbf{M} + \beta\mathbf{K}$ .

Let's assume no damping for simplicity, the results also apply for damped case as the damping matrix is a linear combination of mass and stiffness matrices.

$$\left( s^2 \begin{bmatrix} M_P & M_C^T \\ M_C & M_I \end{bmatrix} + \begin{bmatrix} K_P & K_C^T \\ K_C & K_I \end{bmatrix} \right) \begin{bmatrix} x_P \\ x_I \end{bmatrix} = \begin{bmatrix} F_P \\ 0 \end{bmatrix} \quad (5.2)$$

Here transfer function is defined as  $H(s)x_P = F_P$  and is equal to:

$$H(s) = (s^2 M_P + K_P) - (s^2 M_C + K_C)^T (s^2 M_I + K_I)^{-1} (s^2 M_C + K_C) \quad (5.3)$$

Let

$$K_I = LDL^T \quad (5.4)$$

where  $L$  is lower triangular matrix, and  $D$  is a block-diagonal matrix. If  $K_I$  is positive definite  $D$  may be identity matrix and Cholesky decomposition is used. Define transformation matrix  $X$  as

$$X = \begin{bmatrix} I & 0 \\ -K_I^{-1}K_C & L^{-T} \end{bmatrix} \quad (5.5)$$

$$\begin{aligned} X^T K X &= K' \\ &= \begin{bmatrix} K_P - K_C^T K_I^{-1} K_C & 0 \\ 0 & L^{-1} K_I L^{-T} \end{bmatrix} \\ &= \begin{bmatrix} K'_P & 0 \\ 0 & D \end{bmatrix} \end{aligned} \quad (5.6)$$

$$\begin{aligned}
X^T M X &= M' \\
&= \begin{bmatrix} M'_P & M'_C{}^T \\ M'_C & M'_I \end{bmatrix}
\end{aligned} \tag{5.7}$$

where

$$\begin{aligned}
M'_P &= M_P - K_C^T K_I^{-1} M_C - M_C^T K_I^{-1} K_C + K_C^T K_I^{-1} M_I K_I^{-1} K_C \\
M'_C &= L^{-1} M_C - L^{-1} M_I K_I^{-1} K_C \\
M'_I &= L^{-1} M_I L^{-T}
\end{aligned} \tag{5.8}$$

So the transfer function in terms of the matrices after congruence transformation is

$$H(s) = (s^2 M'_P + K'_P) - (s^2 M'_C)^T (s^2 M'_I + D)^{-1} (s^2 M'_C) \tag{5.9}$$

At this step of algorithm we may continue with two algorithms depending on the positive definiteness of  $K_I$  matrix.

### Case I: $K_I$ is positive definite

Cholesky decomposition is possible  $K_I = LL^T$ , so  $D$  is identity matrix. Let

$$M'_I = V \Lambda V^T \tag{5.10}$$

where  $\Lambda$  is diagonal and has the eigenvalues of  $M'_I$  as its diagonal entries; and columns of  $V$  are the associated eigenvectors such that  $V^T V = I$

Now define the transformation matrix

$$X' = \begin{bmatrix} I & 0 \\ 0 & V \end{bmatrix} \tag{5.11}$$

Then we have the matrices after transformation:

$$K'' = \begin{bmatrix} I & 0 \\ 0 & V^T \end{bmatrix} \begin{bmatrix} K'_P & 0 \\ 0 & I \end{bmatrix} \begin{bmatrix} I & 0 \\ 0 & V \end{bmatrix} \quad (5.12)$$

$$= \begin{bmatrix} K'_P & 0 \\ 0 & I \end{bmatrix}$$

$$M'' = \begin{bmatrix} I & 0 \\ 0 & V^T \end{bmatrix} \begin{bmatrix} M'_P & M'_C{}^T \\ M'_C & M'_I \end{bmatrix} \begin{bmatrix} I & 0 \\ 0 & V \end{bmatrix} \quad (5.13)$$

$$= \begin{bmatrix} M'_P & M'_C{}^T V \\ V^T M'_C & \Lambda \end{bmatrix}$$

$$H(s) = s^2 M'_P + K'_P - s^4 \frac{r_1^T r_1}{1 + \lambda_1 s^2} - s^4 \frac{r_2^T r_2}{1 + \lambda_2 s^2} - \dots \quad (5.14)$$

where  $\lambda_i$  are the eigenvalues and  $r_i$  are the corresponding columns of  $V^T M'_C$ .

Happily we do not need to find all the eigenvalues. There techniques based on Krylov subspace methods which give the eigenvalues in the region of interest. Larger eigenvalues of  $M_I$  correspond to smaller eigenvalues of the system.

## Case II: $K_I$ is not positive definite

We will find an approximation for the transfer function (5.9)

$$H(s) = (s^2 M'_P + K'_P) - (s^2 M'_C)^T (s^2 M'_I + D)^{-1} (s^2 M'_C)$$

Let  $x$  be a solution vector for the following equation:

$$Ax = b \quad (5.15)$$

Let  $\tilde{x} = Vy$  is a solution projection so that

$$\begin{aligned} V^H A \tilde{x} &= V^H b \\ V^H A V y &= V^H b \\ \hat{A} y &= \hat{b} \end{aligned} \quad (5.16)$$

The last equation is a reduced order equation and  $\tilde{x}$  is an approximation to  $x$ .

If we apply this to our problem we have

$$(s^2 M'_I + D)\tilde{x} = M'_C \quad (5.17)$$

where  $\tilde{x}$  is a matrix which we approximate with  $V\bar{y}$ .

$$V^H(s^2 M'_I + D)V\bar{y} = V^H M'_C \quad (5.18)$$

$$(s^2 \Delta_n T_n + \Delta_n)\bar{y} = V^H M'_C \quad (5.19)$$

$$\bar{y} = (s^2 \Delta_n T_n + \Delta_n)^{-1} V^H M'_C \quad (5.20)$$

So  $M'_C{}^T \tilde{x}$  is approximated with

$$M'_C{}^T V (s^2 \Delta_n T_n + \Delta_n)^{-1} V^H M'_C$$

where  $n$  is the number of columns of  $V$ .

Transformation matrix is

$$X' = \begin{bmatrix} I & 0 \\ 0 & V \end{bmatrix} \quad (5.21)$$

In this problem we have real entries in  $V$ .

$$K'' = \begin{bmatrix} I & 0 \\ 0 & V^T \end{bmatrix} \begin{bmatrix} K'_P & 0 \\ 0 & D \end{bmatrix} \begin{bmatrix} I & 0 \\ 0 & V \end{bmatrix} \quad (5.22)$$

$$= \begin{bmatrix} K'_P & 0 \\ 0 & \Delta_n \end{bmatrix}$$

$$M'' = \begin{bmatrix} I & 0 \\ 0 & V^T \end{bmatrix} \begin{bmatrix} M'_P & M'_C{}^T \\ M'_C & M'_I \end{bmatrix} \begin{bmatrix} I & 0 \\ 0 & V \end{bmatrix} \quad (5.23)$$

$$= \begin{bmatrix} M'_P & M'_C{}^T V \\ V^T M'_C & \Delta_n T_n \end{bmatrix}$$



$V$  is obtained using Lanczos Method:

$$V^T(D + s^2 M')V = V^T D(I + s^2 D^{-1} M')V = \Delta_n + s^2 \Delta_n T_n \quad (5.24)$$

$$V^T D(I + s^2 D^{-1} M')V = ?$$

$$D^{-1} M v_1 = \hat{v}_2 = \bar{v}_2 + \alpha_1 v_1 \quad (5.25)$$

$$D^{-1} M v_2 = \hat{v}_3 = \bar{v}_3 + \alpha_2 v_2 + \beta_2 v_1 \quad (5.26)$$

$$D^{-1} M v_3 = \hat{v}_4 = \bar{v}_4 + \alpha_3 v_3 + \beta_3 v_2 + \gamma_3 v_1 \quad (5.27)$$

$$(5.28)$$

$$D^{-1} M v_i = \hat{v}_{i+1} = \bar{v}_{i+1} + \alpha_i v_i + \beta_i v_{i-1} + \gamma_i v_{i-2} + \dots \quad (5.29)$$

$$v_i^T D \hat{v}_{i+1} = \underbrace{v_i^T D \bar{v}_{i+1}}_0 + \alpha_i \underbrace{v_i^T D v_i}_{\delta_i} + \beta_i \underbrace{v_i^T D v_{i-1}}_0 + \dots \quad (5.30)$$

$$\alpha_i = \frac{v_i^T M v_i}{\delta_i} \quad (5.31)$$

$$v_{i-1}^T D \hat{v}_{i+1} = \underbrace{v_{i-1}^T D \bar{v}_{i+1}}_0 + \alpha_i \underbrace{v_{i-1}^T D v_i}_0 + \beta_i \underbrace{v_{i-1}^T D v_{i-1}}_{\delta_{i-1}} + \dots \quad (5.32)$$

$$\beta_i \delta_{i-1} = v_{i-1}^T M v_i \quad (5.33)$$

$$= v_{i-1}^T M D^{-1} D v_i \quad (5.34)$$

$$= \hat{v}_i^T D v_i \quad (5.35)$$

$$= (\bar{v}_i^T + \alpha_{i-1} v_{i-1}^T + \beta_{i-1} v_{i-2}^T + \dots) D v_i \quad (5.36)$$





# Chapter 6

## Examples

In this chapter we will give some examples to demonstrate the speed of the circuit simulation method compared to the FEM solvers. First example is a demonstration of the extraction methods. In all examples, we preferred to use the second method to find the equivalent electrical circuit. The circuits obtained using the first method give the same results.

In these examples, analyses are done using finite element analysis program ANSYS [44](version 5.3), electrical circuit simulation program HSPICE [3](version 97.2), and our in house developed electrical circuit simulation program MAWE [7] which uses asymptotic waveform evaluation method with multi-point moment matching. The simulations are performed on a SPARCstation 20 with 50MHz clock frequency.

### 6.1 Example I

This example is the demonstration of the circuit theoretical method for lossy problems. A spring-mass system with damping is displaced by a distance of  $\Delta = 1\text{in}$  and released (Fig. 6.1). The change of the displacement of the mass during time is examined for 4

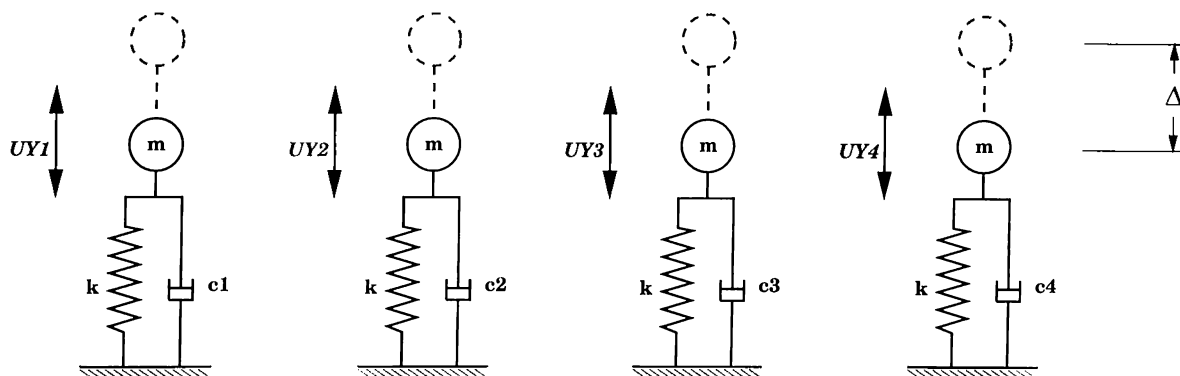


Figure 6.1: Four spring-mass system. (Example I)

damping ratios. 1) Overdamped  $\xi = 2.0$ ; 2) critically damped  $\xi = 1.0$ ; 3) under-damped  $\xi = 0.2$  and 4) undamped  $\xi = 0.0$ .

The equivalent circuit of one damped spring-mass system is given in Fig. 6.2. The other springs have the same L and C values, but the R values are different. As all the springs are standing alone the stiffness, mass and damping matrices are diagonal and there is no coupling between the circuits. Here the current passing through the inductor corresponds to the displacement and the voltage difference across the nodes of the inductor corresponds to the velocity.

The displacement versus time plots obtained by using MAWE are given in Fig. 6.3. The plots exactly match the ones that are obtained from ANSYS.

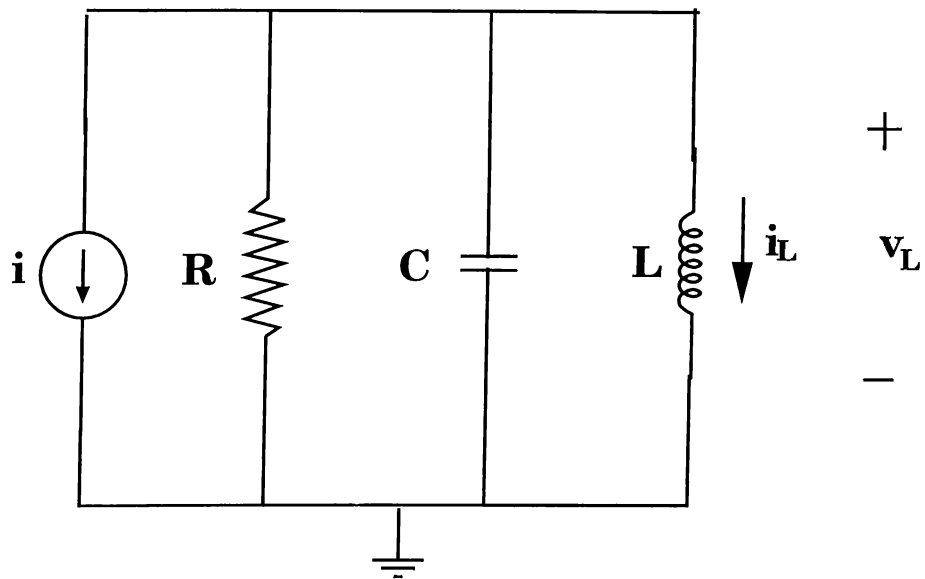


Figure 6.2: Equivalent electrical circuit for a single damped spring-mass system.

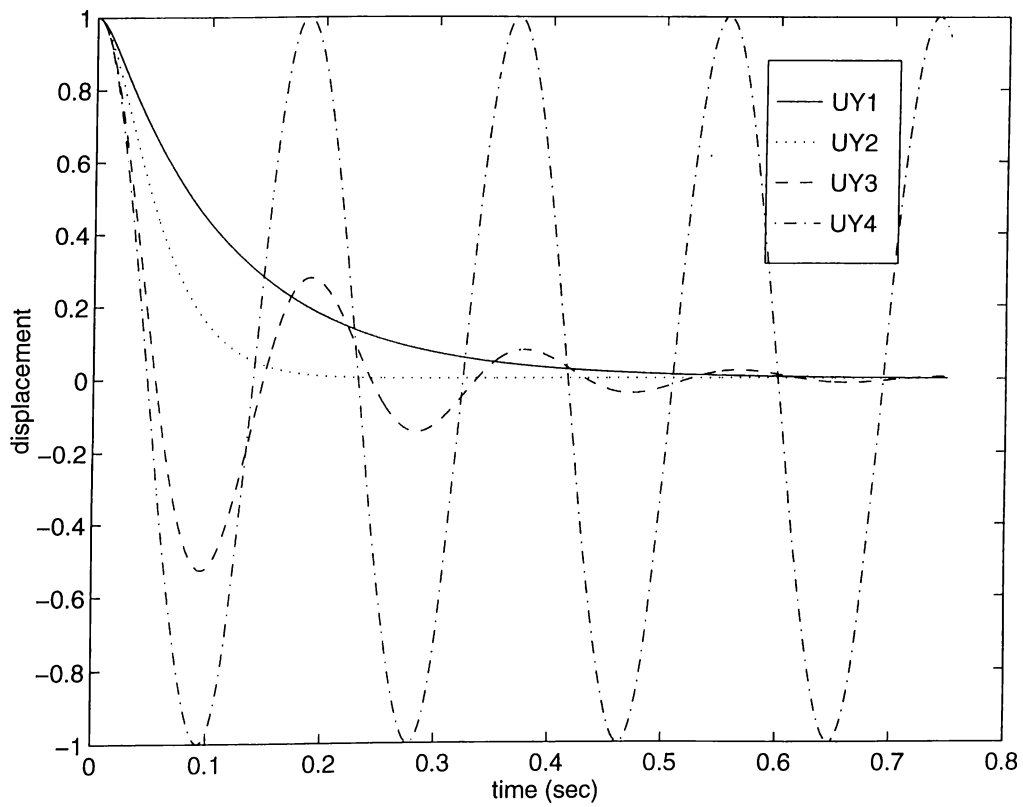


Figure 6.3: Transient analysis results for Example I.

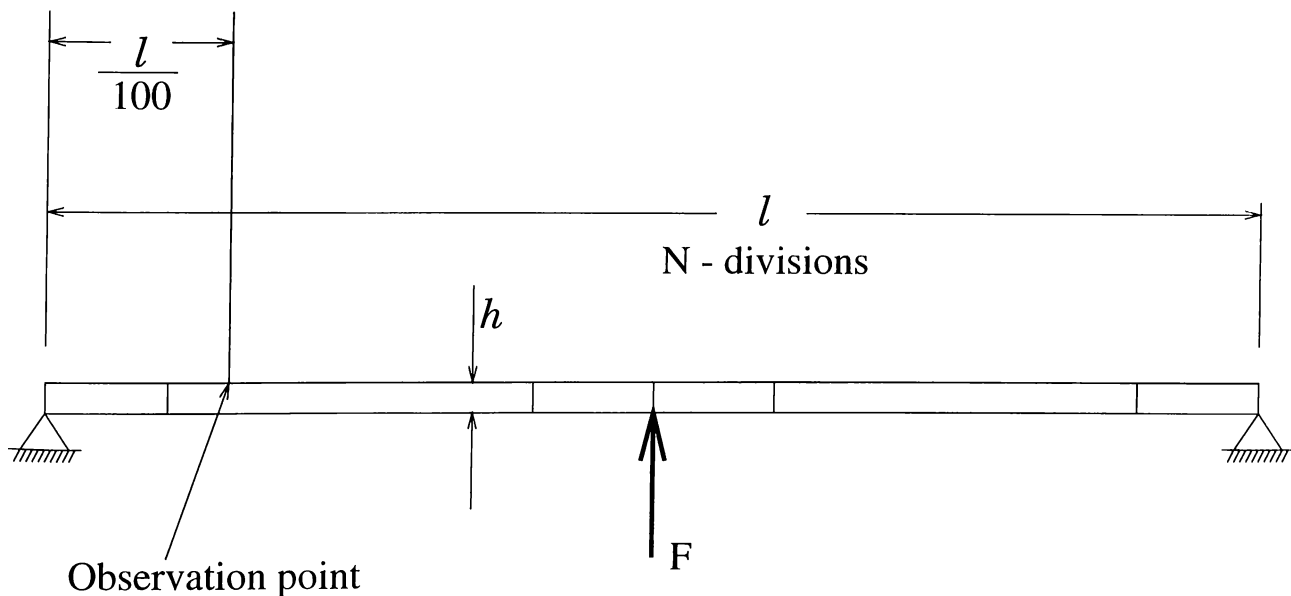


Figure 6.4: Bar supported at the two sides (Example II).

Table 6.1: Circuit summary for Example II.

N	Number of unknowns	L	C	CCCS	VS	Number of circuit nodes	Circuit matrix size
100	200	200	200	1788	400	601	1201
200	400	400	400	3628	800	1201	2401
400	800	800	800	7138	1600	2401	4801

## 6.2 Example II

This example is the harmonic analysis of a simple bar. We have divided the bar into  $N$  elements, apply the force at the mid-point and observe the displacement at  $1/100$  of the length (Fig. 6.4). The system has  $N - 1$  UY unknowns (displacements in  $y$ -direction) and  $N + 1$  ROTZ unknowns (rotations around the  $z$ -axis), which gives a total of  $2N$ . The summary of extracted electrical circuit is given in Table 6.1.

It can be seen in Fig. 6.5 that the harmonic response outputs are indistinguishable. In Table 6.2, execution times during the harmonic analyses are shown (The number of

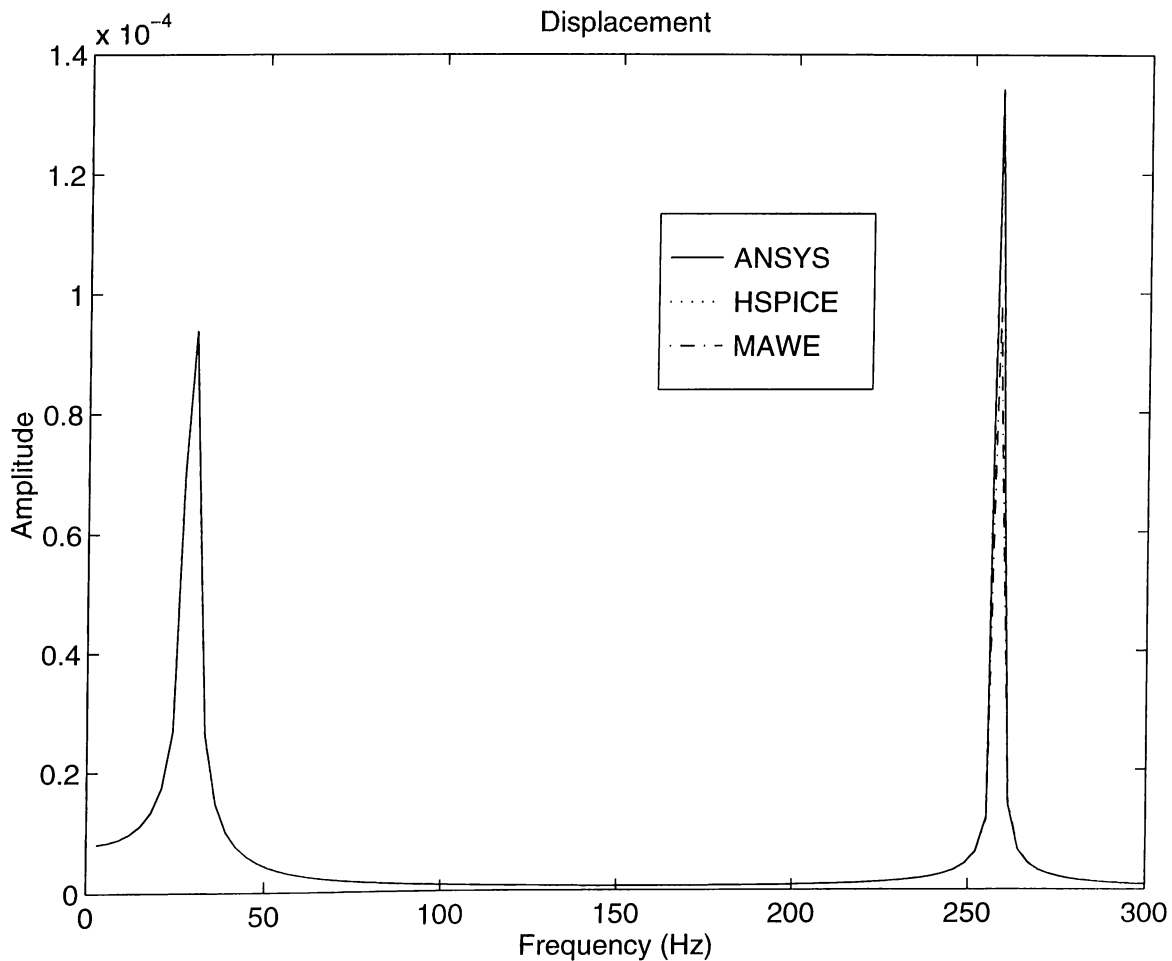


Figure 6.5: Harmonic analysis results for Example II.

expansion points used in MAWE simulation is shown in parentheses). In MAWE analysis 6th order Padé approximation is used, evaluation point is at  $s = 0$ . Electrical solvers do the same job in less time. As  $N$  increases, using electrical solvers becomes even more advantageous. As the body is long and thin the couplings between the displacements are small, and the electrical circuit matrix is sparse. For such problems the speed-up advantage of the circuit theoretical methods is very good.

As the electrical circuit gets larger, HSPICE solution time is better than MAWE. This is probably because the in-house developed sparse matrix solver MAWE is not very efficient for large matrices. Although we use the same electrical circuit netlist file for



Table 6.2: Timing results for Example II (entries are in seconds).

N	Number of frequency points	Execution times		
		ANSYS	HSPICE	MAWE(1)
100	100	57	2.28	1.83
200	100	424	4.83	6.63
400	100	4918	13.80	34.78

both HSPICE and MAWE, the circuit reading time is very small in MAWE compared to that in HSPICE.

In all cases, the output plots are obtained at 100 frequency points. It should be noted that increasing the data points in ANSYS causes a linear increase in the execution time, while the same increase can be achieved at almost no cost in the case of MAWE.

### 6.3 Example III

In this example we analyze the transient behaviour of the bar of Example II. Therefore, the equivalent electrical circuit is the same. A step function with a finite rise time is applied to the mid point of the bar (Fig. 6.4), and the behaviour of the same point in time is simulated. For MAWE, Padé approximation is of order 6; and as the matrix inversion is evaluated only for  $s = 0$ . It can be seen in Fig. 6.6 that all methods give the same results. The execution times are shown in Table 6.3. Again, as the number of unknowns increase, the advantage of using electrical simulators become more significant. For 200 unknowns the speed-up ratios are 1 and 4.4 for HSPICE and MAWE, and for 800 unknowns ratios become 17.5 and 19.4.

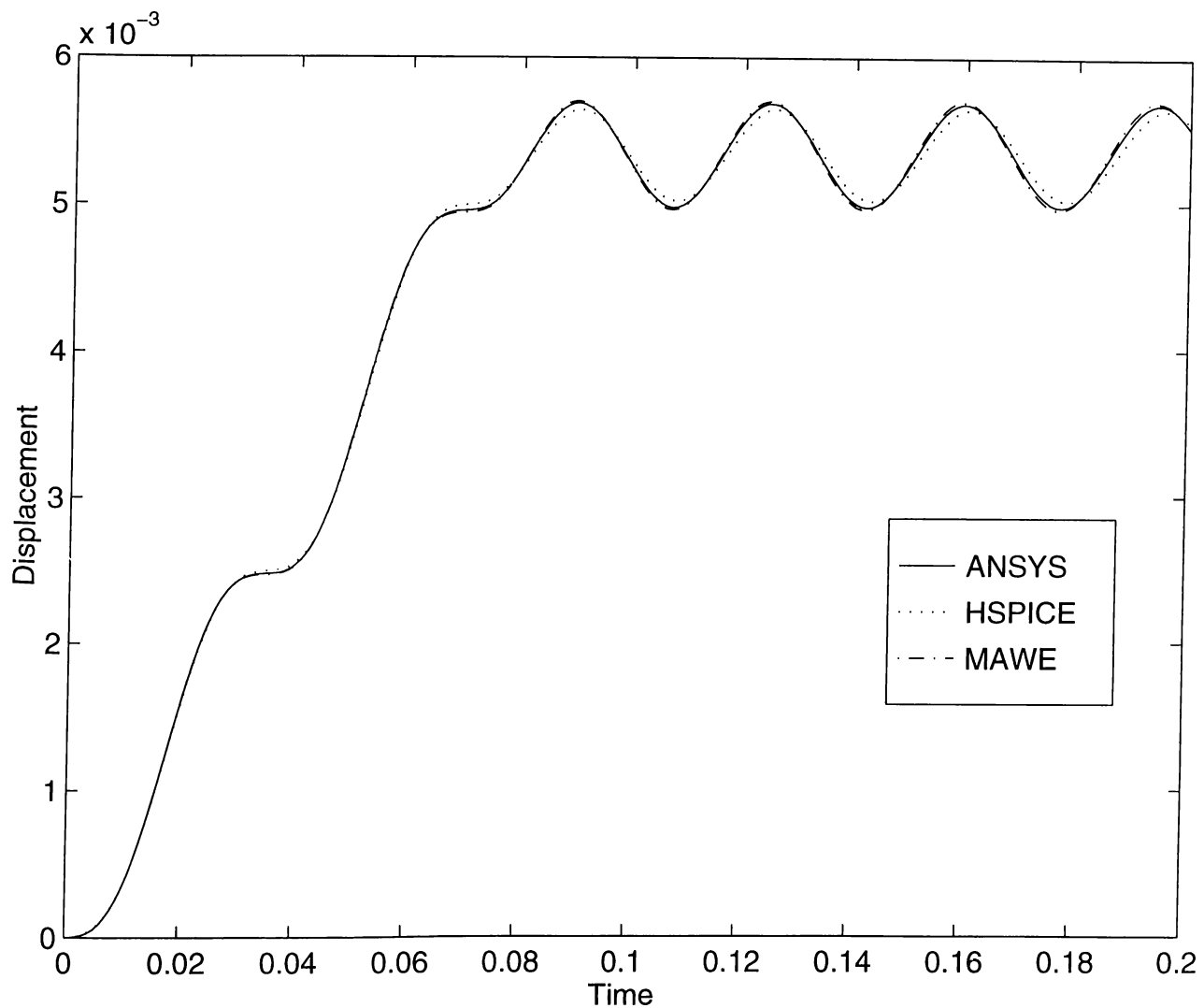


Figure 6.6: Transient analysis results of the three methods for Example III.

Table 6.3: Timing results of the transient analysis in Example III (in seconds).

N	Number of time points	Execution times		
		ANSYS	HSPICE	MAWE(1)
100	200	8.11	8.55	1.84
200	200	76.55	18.25	7.1
400	200	686.01	39.25	35.3

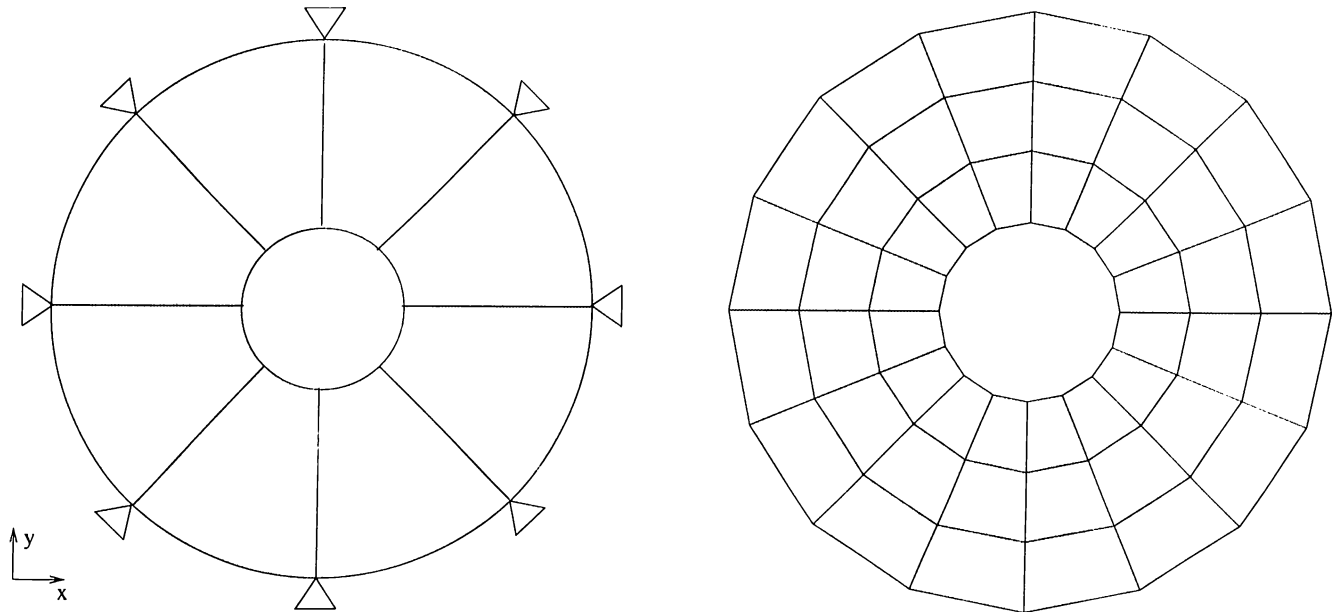


Figure 6.7: Simply supported thin annular plate (Example IV).

## 6.4 Example IV

In this example, the harmonic analysis of a simply supported thin annular plate has been done (Fig. 6.7). The  $x$  and  $y$  components of the displacements, and rotations around the  $z$ -axis are set to 0, and at the outside boundary the translations in the  $z$ -direction and rotations around the radial axis are blocked.

The number of elements along radial direction,  $N1$ , is selected as 5, and the number of elements along circumferential direction,  $N2$ , is chosen to be 32. As a result the number of unknowns is 512. We want to find the harmonic analysis results, when a force is applied at a node at the inside boundary and the frequency response at the same node is observed.

The equivalent circuit has 1537 nodes, 512 inductors, 512 capacitors, 1024 independent voltage sources, 22708 current controlled current sources, and the total matrix size is 3073.

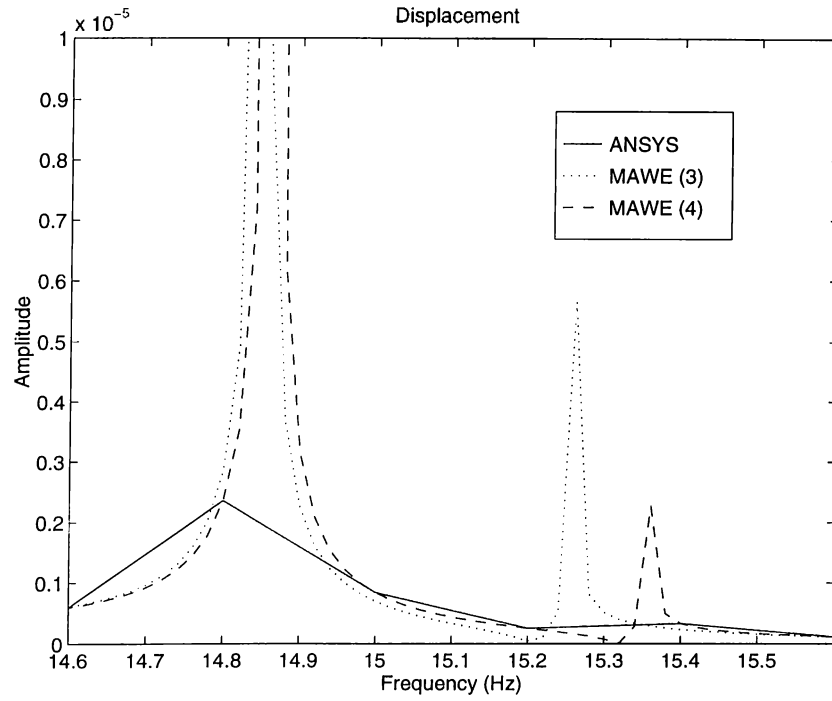


Figure 6.8: Harmonic analysis results around the missing pole in Example IV.

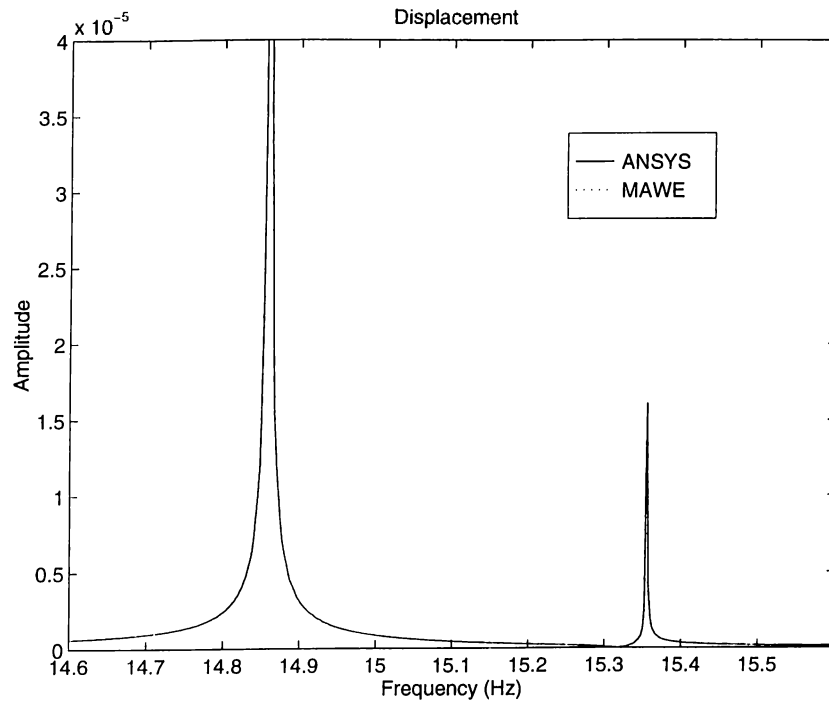


Figure 6.9: Harmonic analysis results around the missing pole in Example IV.

Table 6.4: Timing results for Example IV. (Seconds)

N1	N2	Number of frequency points	Execution times			
			ANSYS	HSPICE	MAWE(3)	MAWE (4)
5	32	100	406.4	67.7	117.3	141.6
5	32	1000	4207	561	119.4	142.8

In 100 point analyses we obtained a rough figure (Fig. 6.8 shows the zoomed version of the result obtained by ANSYS). To have a more accurate result we analyzed the same circuit using MAWE only by changing the number of frequency points to 1000. We saw that in 100-point analyses the pole at 15.3 Hz is missing. At each of the expansion points  $s = 0$ ,  $s = 60i$  and  $s = 120i$ , 12 moments were calculated, and the order of the Padé approximation was 30. In order to locate the pole accurately we increased the number of expansion points by 1. We performed the 1000 point analysis, used 4 expansion points  $s = 0$ ,  $s = 60i$ ,  $s = 90i$ ,  $s = 120i$  and at the expansion points calculated 16, 8, 8, 8 moments respectively. The order of the approximation became 32. To compare the results, harmonic analyses of the same frequency region are done by ANSYS, and MAWE. ANSYS requires 1681.5 seconds for 400 frequency points, while MAWE requires only 54 seconds for 4000 frequency points. The results of the analyses are shown in Fig. 6.9.

The results of the analyses performed for a higher frequency range is shown in Fig. 6.10. Table 6.4 shows the solution times where the numbers of expansion points used in MAWE simulations are shown in parentheses.

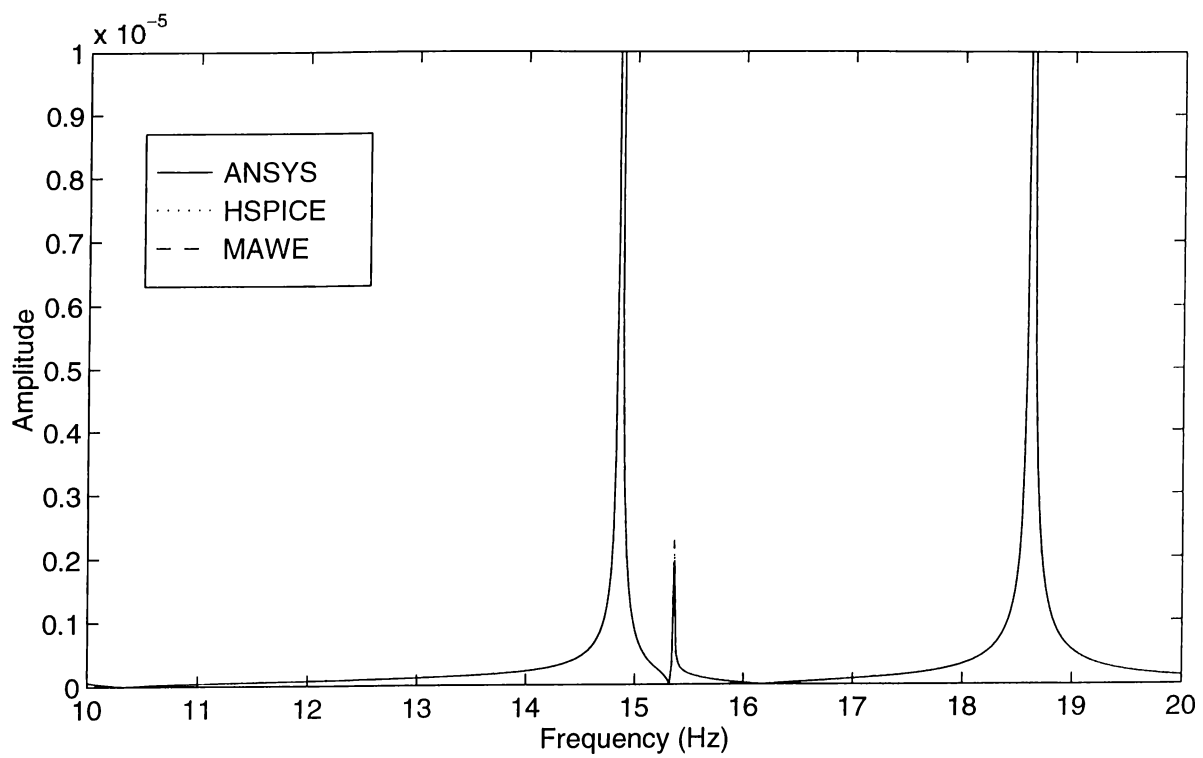
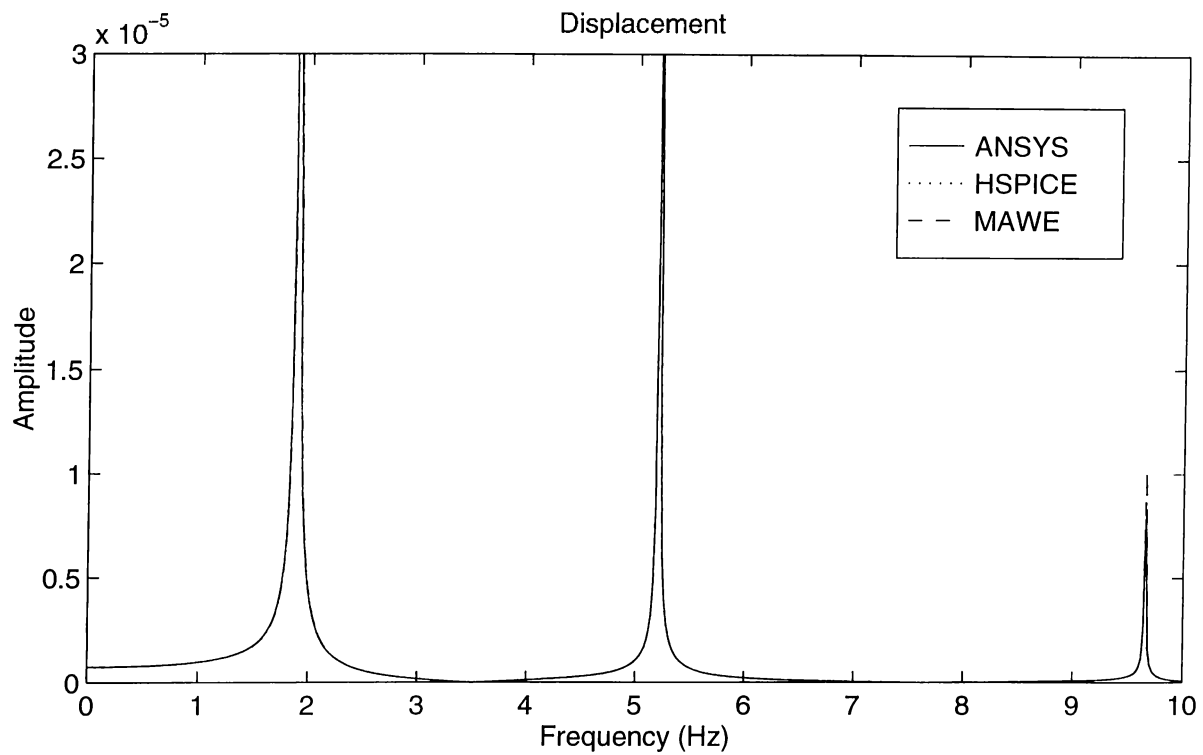


Figure 6.10: Harmonic analysis results of the three methods for Example IV.

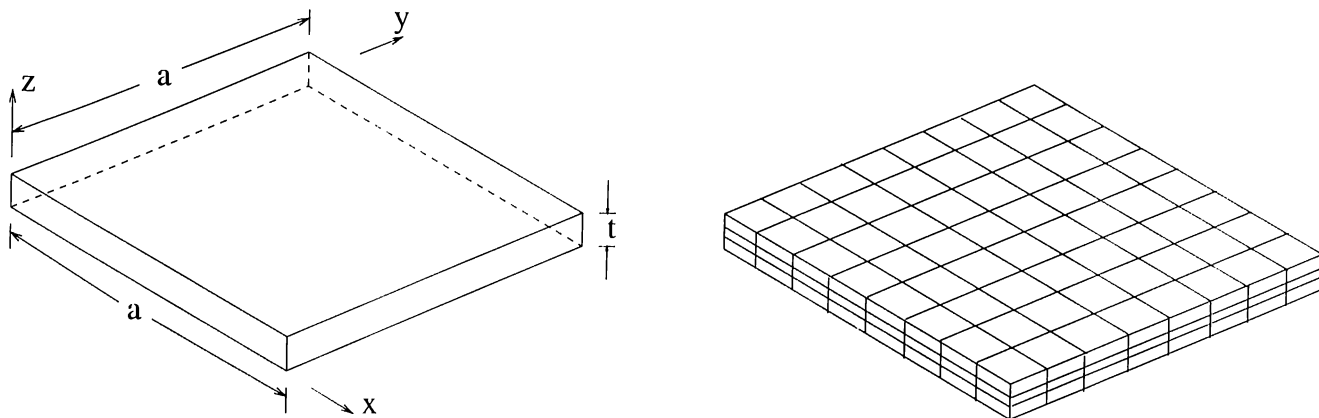


Figure 6.11: Solid square plate supported at one edge (Example V).

## 6.5 Example V

Fifth example is the harmonic analysis of a solid square plate supported at one edge ( $x = 0$  plane in Fig. 6.11), force is applied in the  $y$ -direction at the corner at  $(a,a,0)$ . Displacements in the  $z$ -direction are not allowed, so the displacement has only  $x$  and  $y$  components.

The equivalent circuit has 1729 nodes, 576 inductors, 576 capacitors, 1152 independent voltage sources, 31726 current controlled current sources, and total matrix size is 3457. During the finite element analysis, the body is meshed into  $N1 \times N1$  elements in the  $xy$ -plane and into  $N2$  elements in  $z$  direction. The problem is reduced to 576 unknowns when the constraints are included. The response is observed at point  $(a,0,0)$ . The analyses are done using ANSYS, HSPICE and MAWE. In the first analysis the number of frequency points is 100. The simulation results are shown in Fig. 6.12. The order of the Padé approximation is chosen to be 18, in the second analysis 1024 data points are used in HSPICE and ANSYS simulations. Even in the second analysis the results are not accurate and the pole at 132.88 Hz is missed (Fig. 6.13), so we extended the the data point number to 20480 in MAWE simulation with a cost of few seconds (increase from 285.12 sec. to 292.1 seconds). The *moment number-evaluation point* pairs used in MAWE simulations are shown in Table 6.5.

Table 6.5: Evaluation point-number of moments pairs (Example V).

Evaluation point	number of moments	
0	12	16
800i		8
1200i		8
1600i	12	16
Approx. Order	18	40

In Table 6.7, the time consumptions are shown (the numbers of expansion points used in MAWE simulations are shown in parentheses). Again asymptotic waveform evaluation seemed to be the most efficient analysis tool. When the number of data points is increased, the efficiency becomes more apparent.

For the same example we also applied PACT algorithm with Lanczos tridiagonalization process. PACT algorithm has the same complexity with MAWE which uses one expansion point. We left the input and output nodes as unchanged, so the system has 2 port nodes. Other nodes of the system are considered as internal nodes. We performed 11 Lanczos iterations. As a result we obtained a reduced system with 13 unknowns. We found an equivalent circuit for the reduced system. The new equivalent circuit has 40 nodes (including the reference node), 13 inductors, 13 capacitors, 26 independent voltage sources and 68 current controlled current sources. The total matrix size is reduced to 79. We again used circuit simulators HSPICE and MAWE to analyze the circuit, and obtained a very large drop in circuit simulation time. This time in MAWE we used 3 expansion points which are shown in Table 6.6. The execution times for the reduced system simulations are also included in Table 6.7.



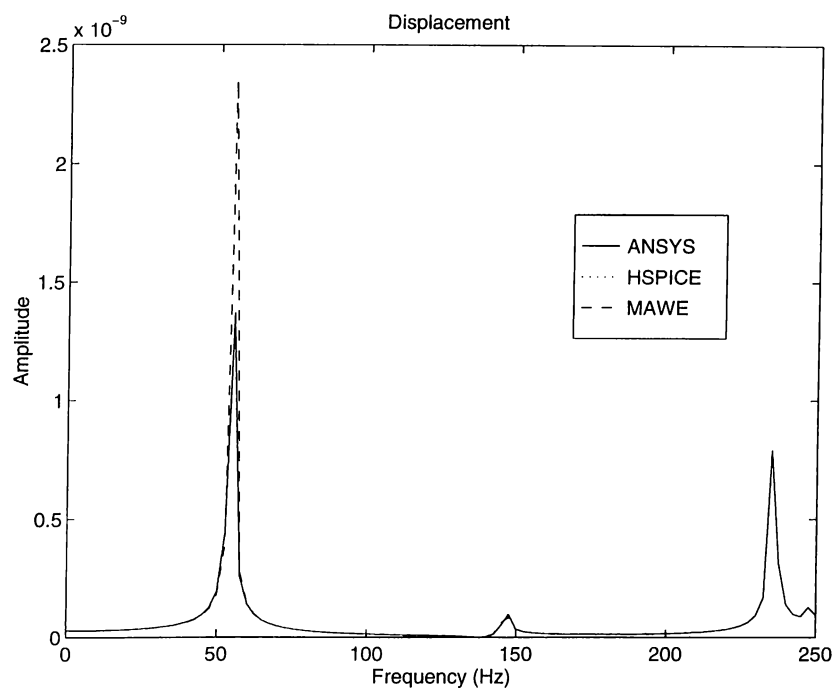


Figure 6.12: Harmonic analysis results of the three methods for Example V.

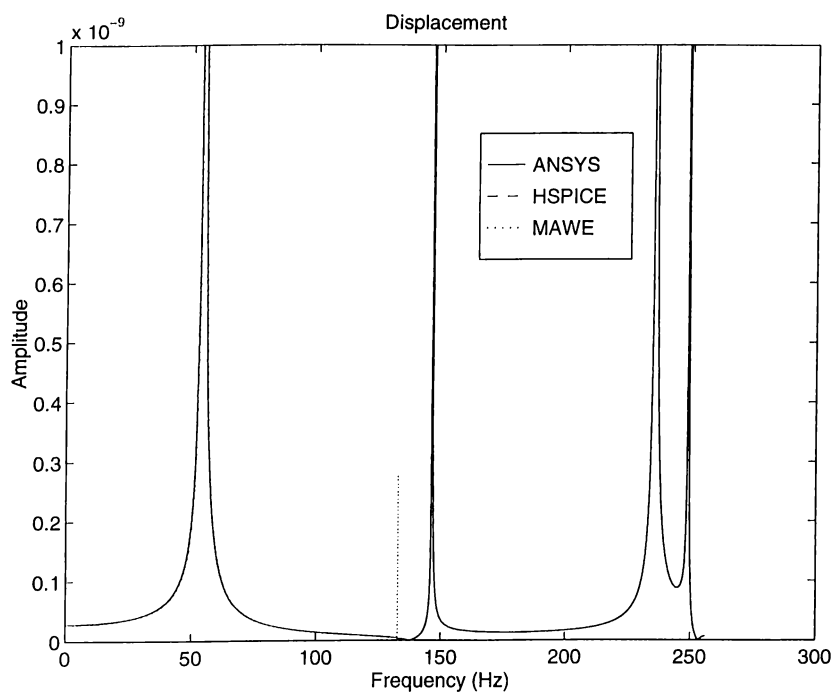


Figure 6.13: More accurate harmonic analysis results for Example V. The pole at 132.88 Hz can only be found by MAWE.

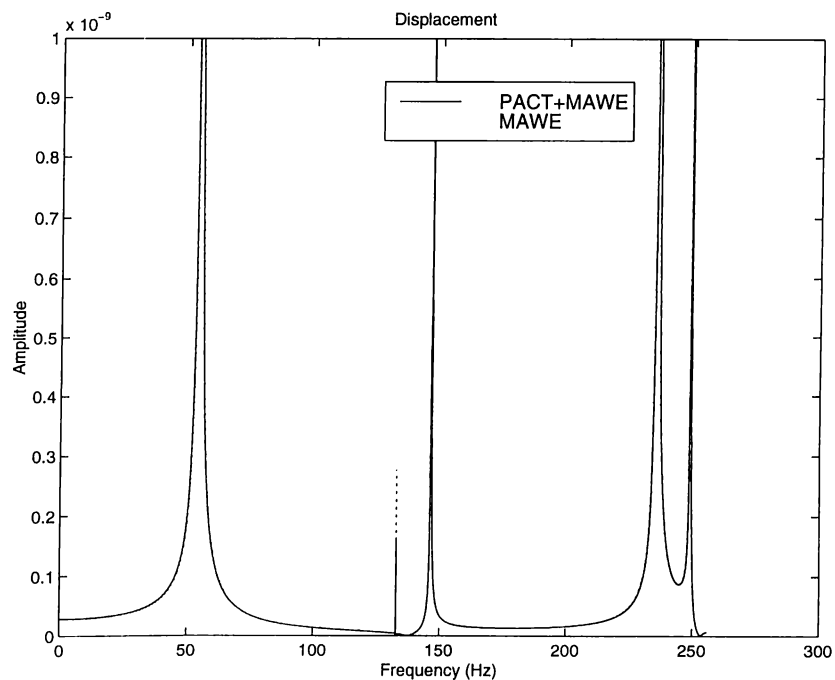


Figure 6.14: Harmonic analysis result using PACT.

Table 6.6: Evaluation point-number of moments pairs for reduced circuit.

Evaluation point	number of moments
0	12
700i	6
1500i	6
Approx. Order	18

Table 6.7: Timing results for Example V (times are in seconds).

N1	N2	Number of unknowns	Number of frequency points	Execution times			
				ANSYS	HSPICE	MAWE(2)	MAWE(4)
8	3	576	100	584.7	288.8	149.4	
8	3	576	1024	5986.4	2576.1	157.9	279.9
8	3	576	20480				291.9

After reduction using PACT			
number of unknowns	frequency points	Execution times	
		HSPICE	MAWE(3)
13	20480	28.5	6

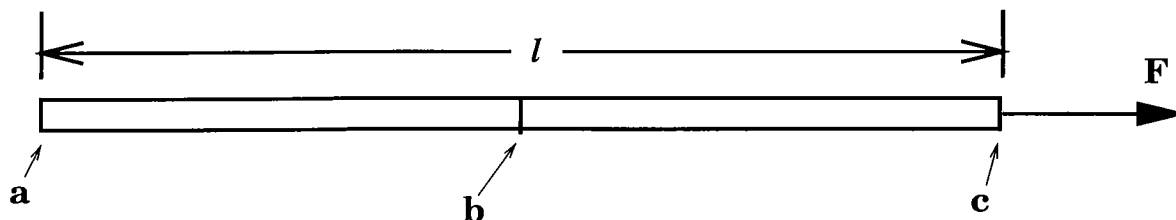


Figure 6.15: The sketch of the problem in Example VI.

## 6.6 Example VI

This example is the simulation of displacement propagation along a bar with free ends Fig. 6.15. The steel bar is 4000 ft long and the displacements and velocities of the ends (nodes **a** and **c**) and the mid-point (node **b**) produced by a sudden force at one end (node **c**) are simulated.

First the structure is divided into 16 elements. The resultant equation of motion problem is solved using ANSYS, HSPICE and MAWE. the fundamental period of the system is 0.48 seconds. First simulations are performed in the first 0.24 second time interval then the simulation time is extended to 1.0 second.

In the simulations ANSYS and HSPICE results are similar, but using MAWE we

lose accuracy with a gain of simulation time. ANSYS and HSPICE solution lasted 2.5 seconds while the required time for MAWE is about 0.6 seconds. For 1000 elements ANSYS requires 249 seconds, HSPICE requires 223 seconds and MAWE requires 22 seconds for the same number of points in time.

The results of the HSPICE simulations for the problem are given in Fig. 6.16. The propagation of the displacement can be seen in the plots.

In figures Fig. 6.17 and Fig. 6.18 the short-time and long-time comparisons of the simulation outputs can be seen.

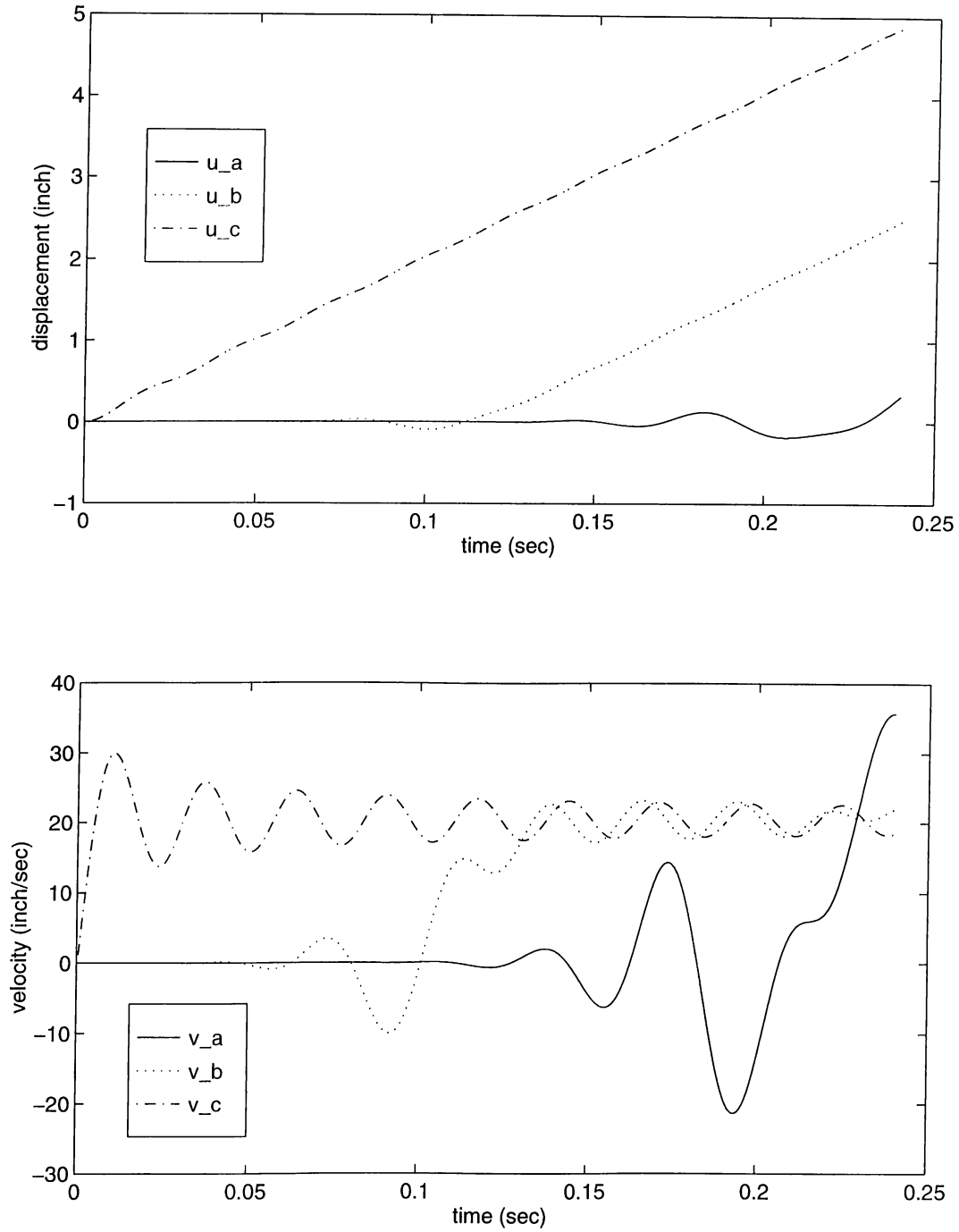


Figure 6.16: The displacement and velocity propagation in the long bar of Example VI.

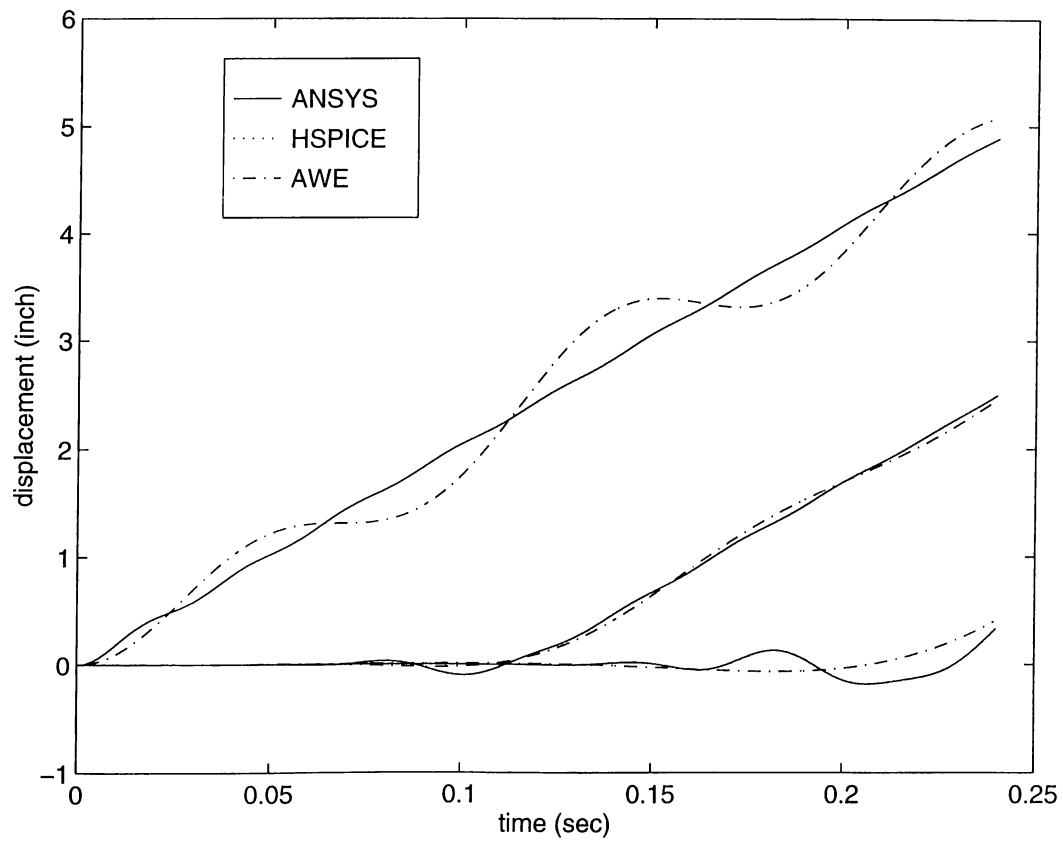


Figure 6.17: Comparison of the results obtained using the three simulators (0.24 sec).

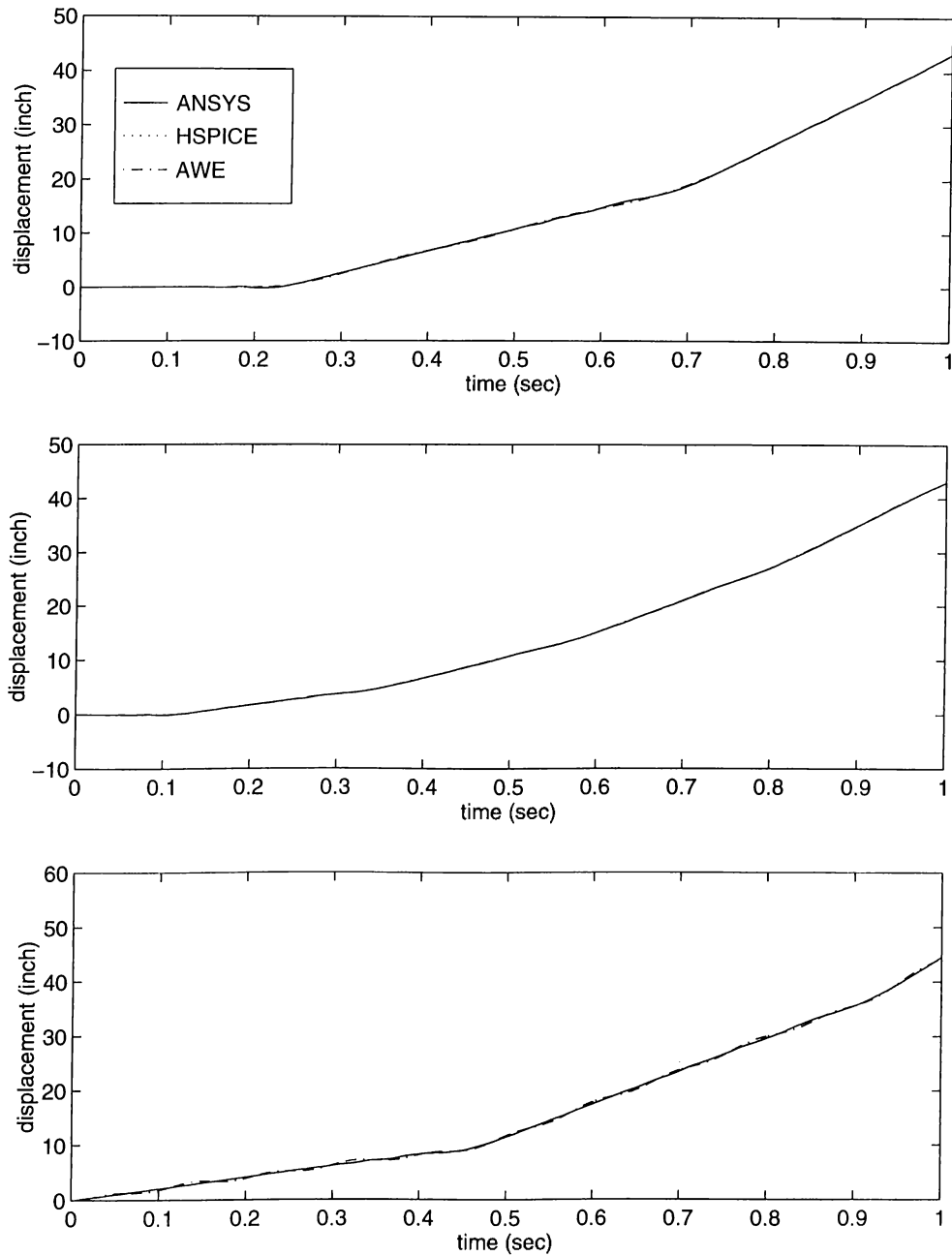


Figure 6.18: Comparison of the results obtained using the three simulators (1 sec).

# Chapter 7

## Conclusions

In this thesis, the analogy between the finite element formulation of the structural mechanics problems and the electrical circuit theory is investigated. Converting structural mechanics problems into circuit analysis problems, we can solve them with a general purpose circuit simulator. Using circuit simulation techniques results in faster solutions for the mechanical problems.

In this work, equivalent circuit extraction is done by a computer program which takes the total mass and stiffness matrices as input and creates an electrical circuit netlist file. In the examples largest netlist is for the last example and the file is built in 1.87 seconds. The resultant circuit matrix is 6 times larger, but the required time for the solution can be very small when fast circuit simulation techniques are used.

One method is using moment matching techniques instead of solving the system of equations at each frequency point. The main reason behind the efficiency of these techniques is the decrease in the number of LU decomposition requirements. Multi-point asymptotic waveform evaluation technique requires one LU decomposition per expansion point. Generally, the number of expansion points is much less than the number of frequency points to get an accurate solution. With a good sparse matrix solver, the



expected speed-up ratio is almost equal to the number of frequency points divided by the number of expansion points. In this study we needed 4 expansion points at most. These expansion points are chosen such that they divide the frequency range of interest into equal portions. We stop dividing if the poles of the main system do not change after including the information of the new expansion point.

Previous work on equivalent circuit construction is mainly dealt with coupled field-circuit problems. These studies are mentioned in Chapter 4. There are two approaches to the problem:

- The part modeled by FEM is solved separately and it is inserted into the circuit as a multiport element.
- Finite elements are converted into elemental equivalent electrical circuits, the whole problem is modeled as an equivalent circuit. The equivalent circuit may have negative valued circuit components, for second order problems inductor loops may occur in lossless cases.

The objective of our study is to solve the full problem using a general circuit simulator. Our method gives no negative valued electrical circuit components, has replaced the couplings with controlled sources, and can be fully solved with a general purpose electrical circuit simulator, so fast circuit solution methods may be applied easily.

In this work, several examples have been studied using the proposed method and an accurate match with the finite element method results has been obtained. Without a significant loss of accuracy, the simulation speed is improved using moment matching techniques.

Another advantage of these techniques, is that the number of data points can be increased without changing the simulation time significantly, and this will decrease the probability of missing high-Q poles.

When there is no damping, the equivalent circuit does not have any resistance values, so the circuit matrix is not diagonally dominant. The sparse solvers employed in solving these circuits can be specially designed to achieve better performance.

Another approach studied in this thesis is the application of a variant of the circuit reduction technique Pole Analysis via Congruence Transformation (PACT). This method is used to obtain passive reduced order models for multi-input multi-output RC networks. It is similar to Component Mode Synthesis (CMS) method, which was developed for structural mechanics problems. In these methods, the unknowns are divided into two subgroups. First group contains the port unknowns which are not reduced. These correspond to the nodes where forces are applied or where the outputs are observed. The second group contains the internal unknowns. The behaviour of these unknowns are simulated using the dominant modes (eigenvectors).

In this study, we use a Lanczos tridiagonalization procedure instead of finding the dominant modes. Then we obtain an equivalent electrical circuit for the reduced model, and solve the circuit using a circuit simulator. Lanczos tridiagonalization process preserves the dominant poles of the system, so it is suitable for finding some of the eigenvalues of very large matrices, and is one of the basic methods used in reduced order modeling of large circuits.

We have seen that using circuit theoretical methods for high speed simulation of structural problems gives very efficient results. The methods employed in this work can be generalized to electromagnetic problems. If the semi-discrete equations of the problem have an order higher than two, special care must be taken as this will increase the number of unknowns.

# Appendix A

## Langrange's Equations

### A.1 Generalized Coordinates

We use the following transformation of a set of  $3N$  cartesian coordinates into a set of  $n$  generalized coordinates.

$$\begin{aligned}x_1 &= f_1(q_1, q_2, \dots, q_n, t) \\x_2 &= f_2(q_1, q_2, \dots, q_n, t)\end{aligned}\tag{A.1}$$

$$x_{3N} = f_{3N}(q_1, q_2, \dots, q_n, t)$$

Assume  $l$  equations of constraints relating  $x$ 's, and  $m$  equations of constraints relating  $q$ 's; so

$$3N - l = n - m = \text{number of degrees of freedom}\tag{A.2}$$

## A.2 Constraints

**Holonomic constraints** are defined as

$$\phi_j(q_1, q_2, \dots, q_n, t) = 0 \quad (j = 1, 2, \dots, m) \quad (\text{A.3})$$

They are called *Scleronomic constraints* when they do not depend explicitly on time, and *Rheonomic constraints* when they are explicit functions of time.

**Nonholonomic constraints** are defined as

$$\sum_{i=1}^n a_{ji} dq_i + a_{jt} dt = 0 \quad (j = 1, 2, \dots, m) \quad (\text{A.4})$$

The equations satisfy the exactness conditions

$$\frac{\partial a_{ij}}{\partial q_k} = \frac{\partial a_{jk}}{\partial q_i} \quad (\text{A.5})$$

$$\frac{\partial a_{ij}}{\partial t} = \frac{\partial a_{jt}}{\partial q_i} \quad (\text{A.6})$$

where  $(i, k = 1, 2, \dots, n)$  and  $j = 1, 2, \dots, m$ .

So another form of (A.4) is:

$$\sum_{i=1}^n a_{ij} \dot{q}_i + a_{jt} = 0 \quad (j = 1, 2, \dots, m) \quad (\text{A.7})$$

## A.3 Virtual Work

$$\delta W = \sum_{j=1}^{3N} F_j \delta x_j \quad (\text{A.8})$$

or

$$\delta W = \sum_{j=1}^N \mathbf{F}_j \cdot \delta \mathbf{r}_j \quad (\text{A.9})$$

where the force  $\mathbf{F}_j$  is applied to a particle whose position vector is  $\mathbf{r}_j$ .

## A.4 Constraint Forces

If the system is subject to constraints, then additional forces are exerted on the particles of the system in order to enforce the constraint conditions. Total virtual work of the internal constraint forces is zero for any rigid body displacement.

## A.5 The Principle of Virtual Work

The necessary and sufficient condition for the static equilibrium of an initially motionless scleronomic system which is subject to workless bilateral constraints is that zero virtual work be done by the applied forces in moving through an arbitrary virtual displacement satisfying the constraints.

The principle of virtual work is of fundamental importance in the study of statics, and if one uses d'Alembert's principle, can be extended to dynamical systems as well.

Consider a system of  $N$  particles in which all the applied forces are conservative.

Potential energy is  $V(x) = V(x_1, x_2, \dots, x_{3N})$ .

The applied force in the direction of  $x_i$  is

$$F_i = -\frac{\partial V}{\partial x_i}$$

Virtual work is

$$\delta W = -\sum_{i=1}^{3N} \frac{\partial V}{\partial x_i} \delta x_i \quad (\text{A.10})$$

Using

$$\delta V = \sum_{i=1}^{3N} \frac{\partial V}{\partial x_i} \delta x_i \quad (\text{A.11})$$

and the principle of virtual work (static equilibrium)

$$\delta V = 0 \quad (\text{A.12})$$

In terms of generalized coordinates

$$\delta V = \sum_{i=1}^n \frac{\partial V}{\partial q_i} \delta q_i \quad (\text{A.13})$$

Since at an equilibrium configuration  $\delta V = 0$  for an arbitrary choice of  $\delta q$ 's, the coefficients are 0. i.e.

$$\frac{\partial V}{\partial q_i} = 0 \quad (i = 1, 2, \dots, n) \quad (\text{A.14})$$

## A.6 D'Alembert's Principle

Newton's Law says that

$$\mathbf{F} - m\mathbf{a} = \mathbf{0} \quad (\text{A.15})$$

Consider a particle with mass  $m$  under a force  $\mathbf{F}$ . The term  $-m\mathbf{a}$  is considered as an inertial force so that the mass is in equilibrium and the problem can be treated as a static problem.

$$\sum_{i=1}^N (\mathbf{F}_i - m\ddot{\mathbf{r}}_i) \cdot \delta \mathbf{r}_i \quad (\text{A.16})$$

## A.7 Generalized Forces

$$\delta W = \sum_{j=1}^{3N} F_j \delta x_j \quad (\text{A.17})$$

$$\delta x_j = \sum_{i=1}^n \frac{\partial x_j}{\partial q_i} \delta q_i \quad (\text{A.18})$$

$\delta t = 0$  as time is assumed to remain constant during virtual displacement.

$$\delta W = \sum_{i=1}^n \underbrace{\sum_{j=1}^{3N} F_j \frac{\partial x_j}{\partial q_i}}_{Q_i} \delta q_i \quad (\text{A.19})$$

where  $Q_i$  is the generalized force associated with the generalized coordinate  $q_i$ .

$$Q_i = -\frac{\partial V}{\partial q_i} \quad (\text{A.20})$$

## A.8 Lagrange's Equations

Kinetic energy

$$T = \frac{1}{2} \sum_{j=1}^{3N} m_j \dot{x}_j^2 \quad (\text{A.21})$$

inserting

$$\dot{x}_j = \sum_{i=1}^n \frac{\partial x_j}{\partial q_i} \dot{q}_i + \frac{\partial x_j}{\partial t} \quad (\text{A.22})$$

we have

$$T = \frac{1}{2} \sum_{k=1}^{3N} m_k \left( \sum_{i=1}^n \frac{\partial x_k}{\partial q_i} \dot{q}_i + \frac{\partial x_k}{\partial t} \right) \left( \sum_{j=1}^n \frac{\partial x_k}{\partial q_j} \dot{q}_j + \frac{\partial x_k}{\partial t} \right) \quad (\text{A.23})$$

$$= \frac{1}{2} \sum_{i=1}^n \sum_{j=1}^n \left( \sum_{k=1}^{3N} m_k \frac{\partial x_k}{\partial q_i} \frac{\partial x_k}{\partial q_j} \right) \dot{q}_i \dot{q}_j$$

$$+ \sum_{i=1}^n \sum_{k=1}^{3N} m_k \frac{\partial x_k}{\partial q_i} \frac{\partial x_k}{\partial t} \dot{q}_i \quad (\text{A.24})$$

$$+ \frac{1}{2} \sum_{k=1}^{3N} m_k \left( \frac{\partial x_k}{\partial t} \right)^2 \quad (\text{A.25})$$

Lets define generalized momentum as

$$p_i = \sum_{j=1}^{3N} m_j \dot{x}_j \frac{\partial \dot{x}_j}{\partial \dot{q}_i} \quad (\text{A.26})$$

Using

$$\frac{\partial \dot{x}_j}{\partial \dot{q}_i} = \frac{\partial x_j}{\partial q_i} \quad (\text{A.27})$$

we obtain

$$p_i = \sum_{j=1}^{3N} m_j \dot{x}_j \frac{\partial x_j}{\partial q_i} \quad (\text{A.28})$$

differentiating  $p_i$

$$\frac{dp_i}{dt} = \sum_{j=1}^{3N} m_j \ddot{x}_j \frac{\partial x_j}{\partial q_i} + \sum_{j=1}^{3N} m_j \dot{x}_j \frac{d}{dt} \left( \frac{\partial x_j}{\partial q_i} \right) \quad (\text{A.29})$$

$$\frac{d}{dt} \left( \frac{\partial x_j}{\partial q_i} \right) = \sum_{k=1}^n \frac{\partial^2 x_j}{\partial q_i \partial q_k} \dot{q}_k + \frac{\partial^2 x_j}{\partial q_i \partial t} = \frac{\partial \dot{x}_j}{\partial q_i} \quad (\text{A.30})$$

$$\frac{dp_i}{dt} = \sum_{j=1}^{3N} m_j \ddot{x}_j \frac{\partial x_j}{\partial q_i} + \frac{\partial T}{\partial q_i} \quad (\text{A.31})$$

The  $m_j \ddot{x}_j$  term is the sum of applied forces  $F_j$  and constraint forces  $R_j$ .

$$\frac{dp_i}{dt} = \underbrace{\sum_{j=1}^{3N} F_j \frac{\partial x_j}{\partial q_i}}_{Q_i} + \underbrace{\sum_{j=1}^{3N} R_j \frac{\partial x_j}{\partial q_i}}_0 + \frac{\partial T}{\partial q_i} \quad (\text{A.32})$$

The second term is 0 as the work done by constraint sources are 0. So we have

$$\frac{d}{dt} \left( \frac{\partial T}{\partial \dot{q}_i} \right) - \frac{\partial T}{\partial q_i} = Q_i \quad (\text{A.33})$$

If the potential energy is such that  $V = V(q, t)$ .

$$\frac{d}{dt} \left( \frac{\partial T}{\partial \dot{q}_i} \right) - \frac{\partial T}{\partial q_i} + \frac{\partial V}{\partial q_i} = 0 \quad (\text{A.34})$$

Define Lagrangian  $L = T - V$ .

$$\frac{d}{dt} \left( \frac{\partial L}{\partial \dot{q}_i} \right) - \frac{\partial L}{\partial q_i} = 0 \quad (\text{A.35})$$

As a general equation we have:

$$\frac{d}{dt} \left( \frac{\partial L}{\partial \dot{q}_i} \right) - \frac{\partial L}{\partial q_i} + \frac{\partial R}{\partial q_i} = Q_i' \quad (\text{A.36})$$

where

$$R = \frac{1}{2} \sum_{i=1}^n \sum_{j=1}^n c_{ij} \dot{q}_i \dot{q}_j. \quad (\text{A.37})$$



is the Rayleigh's dissipation function and is equal to one half of the instantaneous rate of mechanical energy dissipation and  $Q_i'$  are the generalized forces not derivable from a potential function (e.g. friction forces, time-variant forces, nonholonomic constraint force functions).

# Appendix B

## Modal Superposition

Both Modal Superposition method and Component Mode Synthesis method have been developed to reduce computational models in structural dynamics. The main idea is to approximate the solution as a combination of dominant modes. MS is applied to the system as a whole. In the CMS method, reduced models for substructures with fixed interfaces are first developed, then several reduced substructure models are combined into final reduced model. With this definition PACT algorithm may be considered as a variation of this method.

In this section we briefly describe the basics of Modal superposition method.

From Equation (2.11) we have

$$\mathbf{M}\ddot{\mathbf{Q}}(t) + \mathbf{C}\dot{\mathbf{Q}}(t) + \mathbf{K}\mathbf{Q}(t) = \mathbf{P}(t) \quad (\text{B.1})$$

Let the natural frequencies of the undamped eigenvalue problem

$$-\omega^2\mathbf{M}\mathbf{V} + \mathbf{K}\mathbf{V} = 0 \quad (\text{B.2})$$

be given by  $\omega_1, \omega_2, \dots, \omega_n$  ( $\omega = \text{diag}(\omega_i)$ ) with the eigenvectors given by  $\mathbf{v}_1, \mathbf{v}_2, \dots, \mathbf{v}_n$ .

$\mathbf{V}$ , the modal matrix, is defined as

$$\mathbf{V} = \begin{bmatrix} \mathbf{v}_1 & \mathbf{v}_2 & & \mathbf{v}_n \end{bmatrix}$$

Since the eigenvectors are M-orthogonal, we have

$$\mathbf{v}_i^T \mathbf{M} \mathbf{v}_j = \begin{cases} 0 & \text{for } i \neq j \\ 1 & \text{for } i = j \end{cases} \quad (\text{B.3})$$

So for the  $\mathbf{K}$  matrix, we get

$$\mathbf{v}_i^T \mathbf{K} \mathbf{v}_j = \begin{cases} 0 & \text{for } i \neq j \\ \omega_i^2 & \text{for } i = j \end{cases} \quad (\text{B.4})$$

We approximate the solution by a combination of the  $m$  ( $m \leq n$ ) eigenvectors.

$$\vec{\mathbf{Q}}(t) = \sum_{i=1}^m \eta_i(t) \mathbf{v}_i \quad (\text{B.5})$$

Substituting this approximate solution into the equation (B.1), and using

$$\mathbf{C} = \alpha \mathbf{M} + \beta \mathbf{K}$$

we get

$$\ddot{\eta}_i(t) + 2\xi_i \omega_i \dot{\eta}_i(t) + \omega_i^2 \eta_i(t) = N_i(t), \quad i = 1, 2, \dots, m \quad (\text{B.6})$$

where

$$N_i(t) = \mathbf{v}_i^T \vec{\mathbf{P}}(t)$$

and  $\xi_i$ , modal damping ratio, is defined as

$$\xi_i = \frac{\alpha + \beta \omega_i^2}{2\omega_i}$$

# Appendix C

## Modified Node Analysis Formulation

The simplest way of analyzing an electrical linear resistive circuit is to solve for its node voltages with respect to a reference node. Then the branch voltages and branch currents can be calculated easily, if all the elements in the circuit other than current sources are voltage-controlled.

In node analysis, the set of equations are obtained by equating the currents entering the nodes to the currents leaving the nodes. The currents are written in terms of the node voltages.

Modified node analysis (MNA) is based on node analysis, but it is suitably modified so that it can be used on any electrical dynamic circuit. In MNA the variables used are the node voltages with respect to a reference node and the currents in all branches that are not voltage-controlled. The branch equations for these branches are also in the set of equations to be solved. MNA contains small number of unknowns so it is preferred in manual analysis as well as in circuit analysis programs (SPICE, MAWE).

In Table C.1 the branch equations, and in Fig. C.1 the symbols for some electrical circuit components are shown.

Table C.1: Branch equations for the circuit elements

element	abbreviation	branch equation
capacitor	C	$i_C = C \cdot \frac{d}{dt}(v_{n1} - v_{n2})$
inductor	L	$v_{n1} - v_{n2} = L \cdot \frac{d}{dt}(i_L)$
independent voltage source	VS	$v_{n1} - v_{n2} = V$
independent current source	IS	$i = I$
current controlled current source	CCCS	$i = f \cdot i_{cont}$
voltage controlled current source	VCCS	$i = g \cdot (v_{n1_{cont}} - v_{n2_{cont}})$
voltage controlled voltage source	VCVS	$v_{n1} - v_{n2} = e \cdot (v_{n1_{cont}} - v_{n2_{cont}})$
current controlled voltage source	CCVS	$v_{n1} - v_{n2} = h \cdot i_{cont}$

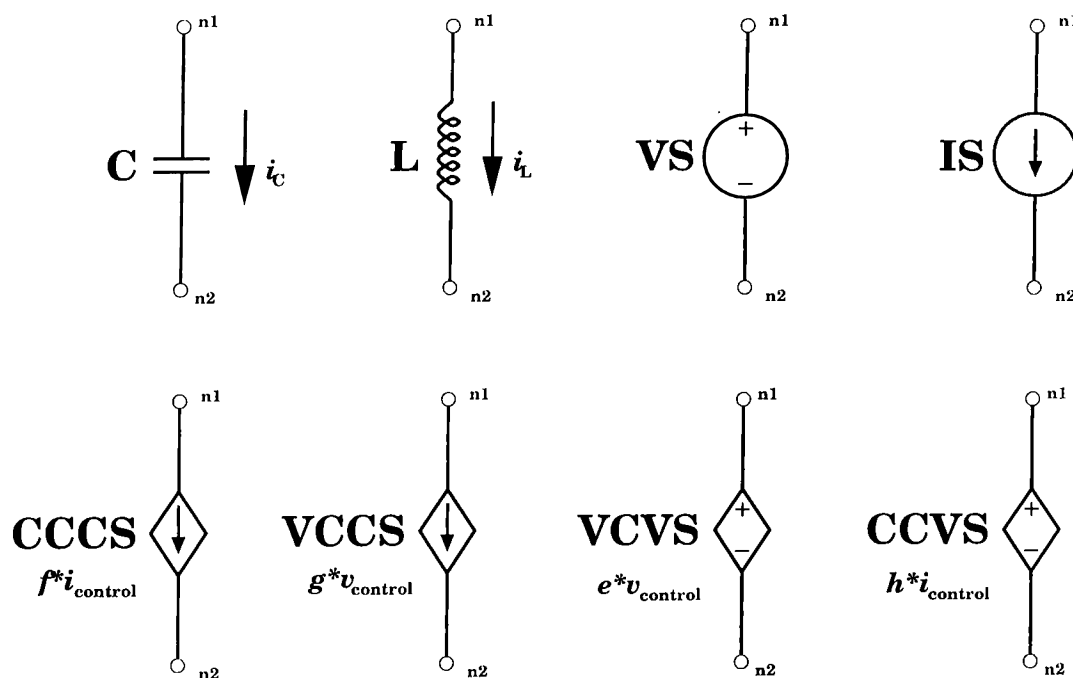


Figure C.1: Symbols for the electrical circuit elements

# Appendix D

## Matlab Codes for PACT

### D.1 PACT

```
function [dof] = pact(infile,outfile,index,option);
%This is the insertion of lanczos method into PACT algorithm.
%
%PACT is pole analysis via congruence transformation.
%
%infile      : input file name
%outfile     : output file name
%index       : the indices of the unknowns which will not change.
%option      : if 0 lanczos method is used,
% if 1 eigen decompostion is used.
% if it does not exist in the arguments assumed to be zero.

%read input
%filename = input('filename = ');
```

```
filename = infile;
if nargin < 4
    option = 0;
end
dof = input('dof = ');

[K,M,F] = readmat(filename,dof);
%keyboard;

n = length(K);
m = length(index);
ind = 1:n;

ind = setdiff(ind,index);

KP = K(index,index);
KC = K(ind,index);
KI = K(ind,ind);

MP = M(index,index);
MC = M(ind,index);
MI = M(ind,ind);

bp = F(index);

%Cholesky decomposition

[L,p] = chol(KI);
```

```

if p==0
disp('Cholesky decomposition is successful. ');
L=L';
D = sparse(eye(size(L)));
else
disp('Cholesky decomposition is not successful, ');
disp('continuing with LDL^t ... ');
[L,D,P] = ld13(KI);
L = P'*L;
end
%keyboard;

%X'KX and X'MX calculations

Linv = inv(L);
A = Linv'*inv(D)*Linv*KC;
B = MC - MI*A;

KP2 = KP - KC'*A;
KI2 = D;

MP2 = MP - A'*MC - B'*A;
MC2 = Linv*B;
MI2 = Linv*MI*Linv';

%Second Step

nn = input('how many eigenvalues? ');

```



```

if (p==0) & option
disp('eigendecomposition will be used.');
```

$$\text{keyboard};$$

```

    [V,Lambda] = eigs(MI2,nn);
delta = sparse(eye(nn));
else
disp('Lanczos method will be used.');
```

$$\text{keyboard};$$

```

[V,delta,Lambda] = newlanc(MC2(:,1),D,L,MI,nn);
Lambda = delta*Lambda;
end

K3 = [KP2 zeros(m,nn); zeros(nn,m) delta];

MC3 = V'* MC2;
M3 = [MP2 MC3'; MC3 Lambda];
F3 = [bp ; zeros(nn,1)];

disp('The reduced model is succesfully obtained,');
disp(['writing to file ',outfile,','.']);
mesg = writemat(outfile,K3,M3,F3);

% =====

function [K,M,C,F] = readmat(filename,dof)
%all the outputs except F are transpose of the real value.

[fid,message] = fopen(filename,'r');
```

```

disp(message);
if prod(size(message)) == 0
K = fscanf(fid,'%f',[dof,dof]);
M = fscanf(fid,'%f',[dof,dof]);
if nargout == 4
    C = fscanf(fid,'%f',[dof,dof]);
    F = fscanf(fid,'%f',[dof,1]);
else
    C = fscanf(fid,'%f',[dof,1]);
end
fclose(fid);
K = sparse(K);
M = sparse(M);
end

% =====
function message = writemat(filename,K,M,C,F)
K = full(K);
M = full(M);
if nargin == 5
    C = full(C);
    F = full(F);
else
F = full(C);
end

dof = length(K);
[fid,message] = fopen(filename,'w');

```

```
if prod(size(message)) == 0
for i=1:dof,
    fprintf(fid, '%.8e ', K(i,1:dof));
        fprintf(fid, '\n');
end
fprintf(fid, '\n');
fprintf(fid, '\n');

for i=1:dof,
    fprintf(fid, '%.8e ', M(i,1:dof));
        fprintf(fid, '\n');
end
fprintf(fid, '\n');
fprintf(fid, '\n');

if nargin == 5
    for i=1:dof,
        fprintf(fid, '%.8e ', C(i,1:dof));
            fprintf(fid, '\n');
    end
    fprintf(fid, '\n');
    fprintf(fid, '\n');
end

fprintf(fid, '%g \n', F);
fclose(fid);
else
disp(message);
```

```
end
```

## D.2 $LDL^T$

```
function [L,D,P] = ldl(A)

alpha = (1 + sqrt(17))/8;
n = length(A); nn = 0; An = A;
pv = 1:n;
L=eye(n);
D = sparse(n,n);
while nn+1<n
[s,p] = piv(An,alpha);
An = An(p,p);
[L1,D1,An] = onestep(An,s);
% keyboard
%update L
if nn >= 1
LL = L(nn+1:n,1:nn);
L = [L(1:nn,1:nn) zeros(nn,n-nn); LL(p,:) L1];

%update D
D = [D zeros(nn,s); zeros(s,nn) D1];
else
L = L1;
D = D1;
end
```

```

%update pv
p = [1:nn p+nn];
pv = pv(p);

nn = nn + s;
end
if nn < n
D = [D zeros(nn,n-nn); zeros(n-nn,nn) An];
end

P = speye(n);
P = P(pv,:);
D = sparse(D);
L = sparse(L);

%=====
function [L,E,D] = onestep(AN,s)
n = length(AN);
% LDL' = PAP'
if n>s
E = AN(1:s,1:s);
C = AN((s+1):n,1:s);
B = AN((s+1):n,(s+1):n);
BB = E\C';
L = [eye(s) zeros(s,n-s); BB' eye(n-s)];
D = B - C*BB;
else

```

```

L = eye(n);
E = AN;
D = [];
end

%=====

function [s,p] = piv(A,alpha)
n = length(A);
[lambda,r] = max(abs(A(2:n,1)));
r = r + 1;

if lambda > 0
if abs(A(1,1)) >= alpha*lambda
s = 1; p=1:n;
else
[sigma,d] = max([abs(A(1:r-1,r)); 0; abs(A(r+1:n,r))]);
if sigma*abs(A(1,1)) >= alpha*lambda^2
s = 1; p=1:n;
elseif abs(A(r,r)) >= alpha*sigma
s = 1; p=[r setdiff(1:n,r)];
else
s = 2; p=[r d setdiff(1:n,[r,d])];
end
end
else
s=1; p = 1:n;

```

```
end
```

### D.3 Lanczos Process

```
function [V,delta,T,err] = newlanc(v1, D, L, M, N)

% V'*(D + sM)*V = delta + s*delta*T
% v1 is the initial vector for the Lanczos process
% N is the number of Lanczos iterations

% this algorithm is implemented by A. Suat Ekinici
% Dec 16, 1998

%initialization

vnew = D\v1;
vold = zeros(size(v1));
dold = 1;
T = sparse(N,N);
V = [];
for i=1:N
eta = norm(vnew);
vn = vnew/eta;
dnew = vn'*D*vn;
bn = eta * dnew/dold;

% vnew = inv(D)*inv(L)*M*inv(L')*vn;
```

```
t = L'\vn;
t = M*t;
vnew = L\t;
vnew = D\vnew;

vnew = vnew - bn* vold;

an = vn'*D*vnew;
an = an/dnew;
vnew = vnew - an*vn;

T(i,i) = an;
delta(i) = dnew;
if i > 1
T(i-1,i) = bn;
T(i,i-1) = eta;
end
vold = vn; dold = dnew;
V = [V vn];
end

if nargout == 4
err = norm(vnew);
end
delta = sparse(diag(delta));
```



## D.4 Solution

```

function [y] = solmec(K,M,F,x,C)
%keyboard;
x = 2*pi*sqrt(-1)*x;
n = length(x);
m = length(K);
y = [];

if nargin == 5
for i = 1:n,
y = [y (M*x(i)*x(i) + C*x(i) + K)\F];
end
else
for i = 1:n,
y = [y (M*x(i)*x(i) + K)\F];
end
end

function [y] = solcirc(G,C,F,x)
x = 2*pi*sqrt(-1)*x;
n = length(x);
m = length(G);
y = [];
for i = 1:n,
y = [y (C*x(i) + G)\F];
end

```

## D.5 Sample Run

### D.5.1 Structural Analysis

```
>> pact('data','red',[1,2,3]);
dof = 512
Cholesky decomposition is successful.
how many eigenvalues? 7
Lanczos method will be used.
```

The reduced model is successfully obtained,  
writing to file red.

```
>> [K,M,F] = readmat('red',10);
>> x = 0:0.02:20;x=x';
>> y = solmec(K,M,F,x);y=y';
>> plot(x,abs(y(:,1)))
```

```
>> pact('data','red',[1,2,3],1);
dof = 512
Cholesky decomposition is successful.
how many eigenvalues? 40
eigendecomposition will be used.
```

The reduced model is successfully obtained,  
writing to file red.

```
>> [K,M,F] = readmat('red',43);
>> y = solmec(K,M,F,x);y=y';
```

```
>> plot(aweh(:,1),aweh(:,2),x,abs(y(:,1)))  
>> exit
```

## D.5.2 Circuit Simulation

```
>> pact('gcf','gcfred',[7,8]);  
dof = 8  
Cholesky decomposition is successful.  
how many eigenvalues? 3  
Lanczos method will be used.
```

The reduced model is successfully obtained,  
writing to file gcfred.

```
>> [G,C,F] = rd('gcfred',5);  
>> x = 0:2e8:2e10;x=x';  
>> y = solcirc(G,C,F,x);y = y';  
>> load rc.dat  
>> plot(rc(:,1),rc(:,2),x,abs(y(:,1)),'r')  
>> quit
```

96351 flops.

# Bibliography

- [1] L. W. Nagel, and D. O. Pederson, “Spice (simulation program with integrated circuit emphasis),” ERL Memo ERL M382, Univ. of California Berkeley, April 1973.
- [2] L. W. Nagel, “Spice2: A computer program to simulate semiconductor circuits,” ERL Memo UCB/ERL M75/520, Univ. of California Berkeley, May 1975.
- [3] META-SOFTWARE, Campbell, CA, *HSPICE User’s Manual*, 1996.
- [4] L. T. Pillage and R. A. Rohrer, “Asymptotic waveform evaluation for timing analysis,” *IEEE Transactions on Computer Aided Design of Integrated Circuits and Systems*, vol. 9, pp. 352–366, April 1990.
- [5] E. Chiprout and M. S. Nakhla, “Analysis of interconnect networks using complex frequency hopping (CFH),” *IEEE Transactions on Computer Aided Design of Integrated Circuits and Systems*, vol. 14, no. 2, pp. 186–200, February 1995.
- [6] M. Celik, O. Ocali, M.A. Tan and A. Atalar, “Pole-zero computation in microwave circuits using multi point Pade approximation,” *IEEE Transactions on circuits and systems-I: Fundamental Theory and Applications*, vol. 42, pp. 6–13, 1995.
- [7] M. Sungur, A.S. Ekinici and A. Atalar, “An efficient program for analysis of interconnect circuits,” *International Journal of Electronics*, vol. 42, pp. 6–13, 1997.

- [8] T. N. Lucas, "Extension of matrix-method for complete multipoint Padé-approximation," *Electronics Letters*, vol. 29, no. 20, pp. 1805–1806, 1993.
- [9] G. Kron, "Equivalent circuits of the elastic field," *Journal of Applied Mechanics*, vol. 11, pp. A149–A161, September 1944.
- [10] G. K. Carter, "Numerical and network analyzer solution for the equivalent circuits for the elastic field," *Journal of Applied Mechanics*, vol. 11, pp. A162–A167, September 1944.
- [11] Jia Tzer Hsu and Loc Vu-Quoc, "A rational formulation of thermal circuit models for electrothermal simulation— part I: Finite element method," *IEEE Transactions on Circuits and Systems—1: Fundamental Theory and Applications*, vol. 43, no. 9, pp. 721–732, September 1996.
- [12] J. T. Hsu and L. V. Quoc, "A rational formulation of thermal circuit models for electrothermal simulation— part II: Model reduction techniques," *IEEE Transactions on Circuits and Systems—1: Fundamental Theory and Applications*, vol. 43, no. 9, pp. 733–744, September 1996.
- [13] I. A. Tsukerman, A. Konrad, G. Menuier and J. C. Sabonnadière, "Coupled field circuit problems: Trends and accomplishments," *IEEE Transactions on Magnetics*, vol. 29, no. 2, pp. 1701–1704, March 1993.
- [14] F. Piriou and A. Razek, "Finite element analysis in electromagnetic systems accounting for electric circuits," *IEEE Transactions on Magnetics*, vol. 29, no. 2, pp. 1669–1675, March 1993.
- [15] S. J. Salon, L. Ovacik and J. F. Balley, "Finite element calculation of harmonic losses in ac machine windings," *IEEE Transactions on Magnetics*, vol. 29, no. 2, pp. 1442–1445, March 1993.

- [16] A. Nicolet, F. Delincé, N. Bamps, A. Genon and W. Legros, “A coupling between electric circuits and 2d magnetic field modeling,” *IEEE Transactions on Magnetics*, vol. 29, no. 2, pp. 1697–1700, March 1993.
- [17] J. S. Wang, “A nodal analysis approach for 2d and 3d magnetic-circuit coupled problems,” *IEEE Transactions on Magnetics*, vol. 32, no. 3, pp. 1074–1077, May 1996.
- [18] G. Bedrosian, “A new method for coupling finite element field solutions with external circuits and kinematics,” *IEEE Transactions on Magnetics*, vol. 19, no. 2, pp. 1664–1668, March 1993.
- [19] J. Väänänen, “Circuit theoretical approach to couple two-dimensional finite element models with external circuit equations,” *IEEE Transactions on Magnetics*, vol. 32, no. 2, pp. 400–410, March 1996.
- [20] Z. W. Shi and C. B. Rajanathan, “A method of approach to transient eddy current problems coupled with voltage sources,” *IEEE Transactions on Magnetics*, vol. 32, no. 3, pp. 1082–1085, May 1996.
- [21] T. E. McDermott, P. Z. and J. Gilmore, “Electromechanical system simulation with models generated from finite element solutions,” *IEEE Transactions on Magnetics*, vol. 33, no. 2, pp. 1682–1685, March 1997.
- [22] B. A. Auld, *Acoustic Fields and Waves in Solids*, vol. I, R.E. Krieger Publishing Company, Malabar FL, 2nd edition, 1990.
- [23] J. Gong and J. L. Volakis, “Awe implementation for electromagnetic analysis,” *Electronics Letters*, vol. 32, no. 24, pp. 2216–2217, November 1996.
- [24] M. A. Kolbehdari, M. Srinivasan, M. S. Nakhla, Q. J. Zhang, and R. Achar, “Simultaneous time and frequency domain solutions of em problems using finite element

- and cfh techniques,” *IEEE Transactions on Microwave Theory and Techniques*, vol. 44, no. 9, pp. 1526–1534, September 1996.
- [25] D. Skoogh, *Krylov subspace methods for linear systems, eigenvalues and Model Order Reduction*, Ph.D. thesis, Chalmers University of Technology, Department of Mathematics, Göteborg Sweden, December 1998.
- [26] B. N. Parlett and D. S. Scott, “The lanczos algorithm with selective orthogonalization,” *Mathematics of Computation*, vol. 33, no. 145, pp. 217–238, January 1979.
- [27] T. S. Zheng, W. M. Liu and Z. B. Cai, “A generalized inverse iteration method for solution of quadratic eigenvalue problems in structural dynamic analysis,” *Computers and Structures*, vol. 33, no. 5, pp. 1139–1143, 1989.
- [28] C. Rajakumar and C. R. Rogers, “The lanczos algorithm applied to unsymmetric generalized eigenvalue problem,” *International Journal for Numerical Methods in Engineering*, vol. 32, pp. 1009–1026, 1991.
- [29] C. Rajakumar, “Lanczos algorithm for the quadratic eigenvalue problem in engineering applications,” *Computer Methods in Applied Mechanics and Engineering*, vol. 105, pp. 1–22, 1993.
- [30] C. Rajakumar and A. Ali, “Acoustic boundary element eigenproblem with sound absorption and its solution using lanczos algorithm,” *International Journal for Numerical Methods in Engineering*, vol. 36, pp. 3957–3972, 1993.
- [31] I. W. Lee, M. C. Kim, A. R. Robinson, “Efficient solution method of eigenproblems for damped structural systems using modified newton-raphson technique,” *Journal of Engineering Mechanics*, vol. 124, no. 5, pp. 576–580, May 1998.
- [32] P. Feldmann and R. W. Freund, “Efficient linear circuit analysis by pade approximation via the lanczos process,” *IEEE Transactions on Computer Aided Design of Integrated Circuits and Systems*, vol. 14, pp. 639–649, May 1995.

- [33] R. W. Freund and P. Feldmann, “Reduced order modeling of large passive linear circuits by means of the sypvl algorithm,” Numerical Analysis Manuscript, Bell Laboratories, Murray Hill, New Jersey, 1996.
- [34] P. Feldmann and R. W. Freund, “Reduced order modeling of large linear subcircuits via a block lanczos algorithm,” in *32nd ACM/IEEE Design Automation Conference*, 1995.
- [35] J. I. Aliaga, D. L. Boley, R. W. Freund and V. Hernández, “A lanczos-type method for multiple starting vectors,” Numerical Analysis Manuscript, Bell Laboratories, Murray Hill, New Jersey, 1996.
- [36] R. W. Freund and P. Feldmann, “The sypvl algorithm and its applications to interconnect simulation,” Numerical Analysis Manuscript, Bell Laboratories, Murray Hill, New Jersey, 1997.
- [37] R. W. Freund and P. Feldmann, “Reduced order modeling of large linear passive multi-terminal circuits using matrix-padé approximation,” Numerical Analysis Manuscript, Bell Laboratories, Murray Hill, New Jersey, 1997.
- [38] A. Odabasioglu, M. Celik and L. T. Pileggi, “PRIMA: Passive reduced-order interconnect macromodelling algorithm,” *IEEE Transactions on Computer Aided Design of Integrated Circuits and Systems*, vol. 17, no. 8, pp. 645–654, August 1998.
- [39] K. J. Kerns and A. T. Yang, “Stable and efficient reduction of large, multiport rc networks by pole analysis via congruence transformations,” *IEEE Transactions on Computer Aided Design of Integrated Circuits and Systems*, vol. 16, no. 7, pp. 734–744, July 1997.
- [40] K. J. Kerns and A. T. Yang, “Preservation of passivity during RLC network reduction via split congruence transformations,” *IEEE Transactions on Computer Aided Design of Integrated Circuits and Systems*, vol. 17, no. 7, pp. 582–591, July 1998.



- [41] R. W. Freund, "Reduced order modeling techniques based on krylov subspaces and their use in circuit simulation," Numerical Analysis Manuscript, Bell Laboratories, Murray Hill, New Jersey, 1998.
- [42] O. C. Zienkiewicz and R. L. Taylor, *The Finite Element Method*, vol. I, Basic Formulation and Linear Problems, McGraw-Hill Book Company, London, 4th edition, 1989.
- [43] S. S. Rao, *The Finite Element Method in Engineering*, Pergamon Press, Oxford, 2nd edition, 1989.
- [44] ANSYS, Inc., *ANSYS Help System and Documentation*, 1995.
- [45] D. T. Greenwood, *Principles of Dynamics*, Prentice-Hall, Inc., Englewood Cliffs, N.J., 2nd edition, 1988.
- [46] L. O. Chua, C. A. Desoer and E. S. Kuh, *Linear and Nonlinear Circuits*, Series in electrical engineering. McGraw-Hill, New York, 1987.
- [47] T. K. Tang and M. S. Nakhla, "Analysis of high-speed vlsi interconnects using the asymptotic waveform evaluation technique," *IEEE Transactions on Computer Aided Design of Integrated Circuits and Systems*, vol. 11, no. 3, pp. 341-352, March 1992.
- [48] C. T. Dikmen, "BUSTLE: A new circuit simulation tool using asymptotic waveform evaluation and piece-wise linear approach," M.S. thesis, Bilkent University, Dept of Electrical and Electronics Eng., Bilkent, Ankara, Turkey, July 1990.
- [49] S. Topcu, *PLAWE: A piecewise linear circuit simulator using asymptotic waveform evaluation*, Ph.D. thesis, Bilkent University, Dept of Electrical and Electronics Eng., Bilkent, Ankara, Turkey, July 1994.
- [50] E. Chiprout and M. S. Nakhla, *Asymptotic Waveform Evaluation and Moment Matching for Interconnect Analysis*, Kluwer Academic Publishers, 1994.

- [51] O. Ocali, M. A. Tan, and A. Atalar, "A new method for nonlinear circuit simulation in time domain: Nowe," *IEEE Transactions on Computer Aided Design of Integrated Circuits and Systems*, vol. 15, no. 3, pp. 368–374, March 1996.
- [52] M. Alaybeyi, "BUSTLE: A new circuit simulation tool," M.S. thesis, Bilkent University, Dept of Electrical and Electronics Eng., Bilkent, Ankara, Turkey, July 1990.
- [53] *Analogy Inc.*, Beaverton OR.

# Vita

Ahmet Suat Ekinçi was born in Burdur, Turkey, in 1969. He received his B.Sc. and M.Sc. degrees from Bilkent University, Ankara, Turkey, in 1991 and 1994, respectively, both in electrical and electronics engineering. His current research interests include design and simulation of VLSI circuits, high speed circuit simulation techniques and model order reduction.